Hydrolysis, Solvation, and Reduction of SO_3, S_2O_6, $ClO_3(OH)$, Cl_2O_7, and ArO_4—Relating Chemical Properties to the Instability of S═O, Cl═O, and Ar═O Groups

J. R. Tobias Johnson*

Inorganic Chemistry, Department of Chemistry, Göteborg University, S-412 96 Göteborg, Sweden

Itai Panas

Department of Inorganic Environmental Chemistry, Chalmers University of Technology,
S-412 96 Göteborg, Sweden

Received: July 6, 2001; In Final Form: October 23, 2001

Successive water addition to the mononuclear species SO_3(g) and $ClO_3(OH)$(g) and ArO_4(g), as well as the binuclear clusters S_2O_6(g) and Cl_2O_7(g), is studied by means of quantum chemistry. A large basis set effect is observed for the S−O, Cl−O, and Ar−O bond distances, as well as for redox energetics. While the 6-311+G(d,p) basis set is enough for O and H atoms, S, Cl, and Ar require the 6-311+G(3df) set for an accurate description. Given this combination of basis sets, B3LYP is found to give very good results of equal quality to high-level methods. The dominating chemical feature that is monitored is the instability of the S═O, Cl═O, and Ar═O bonds. This instability causes the acidity displayed by water solutions of $SO_2(OH)_2$ and $ClO_3(OH)$ and makes the Cl and Ar systems prone to O_2(g) evolution. The latter system is also reduced directly by water, while the reduction of $SO_2(OH)_2$ to H_2S requires a reducing agent of equivalent power to H_2. Three water ligands are necessary to produce nanoscale deprotonation of $SO_2(OH)_2$ and $ClO_3(OH)$. The hydrolytic cleavage of the S−O−S and Cl−O−Cl bridges is exothermic by 23−30 kJ/mol, which explains the sensitivity to excess of water displayed by these polymers.

Introduction

Acidity and redox stability have emerged as the main two chemical properties for characterizing a chemical substance. For compounds where the oxidation state of a certain element is thermodynamically unstable toward redox reactions, the actual stability depends on the magnitude of the activation energy for the conversion and the absence of catalysts or redox agents. The ability of an element to acquire a high oxidation state is reflected in the number and charge of the counterion ligands that it can accommodate. The two main factors that control coordination are ionic radius and valence shell flexibility. In case of light central ions (e.g., 3p-elements), the tetrahedral coordination has been found to dominate. Four electron pairs can be accommodated in the four sp^3 hybrids of the valence orbitals, which produces a tetrahedral coordination. The stable octahedral coordination of e.g., SF_6(g) reflects the extension of the valence to include d-orbitals.[1] This occurs by the formation of sp^3d^2 hybrid orbitals, which can accept six electron pairs of local σ symmetry. Additional flexibility to this type of bonding is introduced for the d-elements, e.g., in $Ni(CO)_6$, which also has contributions from the π^* orbitals of the ligands by means of back-donation from the filled t_{2g} components of the d-shell.

The present work is the third part of a comprehensive investigation which addresses the water chemistry of the main molecular oxides of all the 3p elements. Thus, in a first study, the trivalent AlO(OH) and Al_2O_3 systems were allowed to react with water.[2] The final product was found to be a binuclear hydroxide or a hydrated complex of such a species. A second investigation addressed the water chemistry of the $Si(OH)_4$ and $PO(OH)_3$ systems and their binuclear anhydride forms.[3] In the water complexes of $PO(OH)_3$, the formation of hydrogen-bonded water bridges between P−OH and P═O groups was preferred. Proton delocalization in such a bridges comprises the primary step in the proton release of phosphoric acid. No such effect was seen for $Si(OH)_4$, which is consistent with the much higher pK_a value of the latter. Hydrolysis of the Si−O−Si and P−O−P bridges were found to be slightly endothermic, consistent with the tendency for aggregation found in case of aluminum.

In the present study, we will focus on the oxides of the 3p elements sulfur, chlorine, and argon. The tetrahedron comprises a common oxygen coordination body for the first two in sulfuric acid and perchloric acid. The high oxidation states of S and Cl, VI and VII, respectively, in conjunction with high lying and 3d states suggest that these systems are susceptible to reduction. The issues raised in the present study include (i) possible channels for decomposition of H_2SO_4 and $HClO_4$ molecules, (ii) what lends these bulk chemicals their redox stabilities, and (iii) to what extent their acidities reflect their high oxidation states.

H_2SO_4, SO_3, and H_2O represent the three dominating species in the world's single most important bulk chemical, sulfuric acid. The crucial step in stabilizing the acid in general as well as in industrial production consists of hydrating SO_3(g). This gas is produced by oxidation of S(s). Critical to this oxidative scheme is the conversion of SO_2(g) into SO_3(g), which can be reversed or slowed, depending on reaction conditions. The main product from the reduction of solid sulfur is H_2S(g). This molecule comprises a main ingredient in biological synthesis of cysteine and the biological metal sulfides, e.g., ferredoxines. Thus, exploring redox systems, which represent conversions between the common oxidation states of S, i.e., −II, 0, +IV, and +VI, becomes highly desirable. The water chemistry and

10.1021/jp015502t CCC: $22.00

protolytic properties of $SO_2(OH)_2$ constitute a second area of interest. Condensation of sulfuric acid into polymeric chains according to R1 is known to account for the high viscosity of concentrated sulfuric acid

$$nH_2SO_4(l) \leftrightarrow H_2(SO_3)_n(l) + (n-1)H_2O(l) \qquad (R1)$$

It thus becomes interesting to study the stability of the S−O−S bridges toward hydrolysis. A balanced description of both the binuclear and mononuclear species in this system requires a consistent understanding of the solvent−solute interactions. The exact nature of this interplay can be clarified through investigations on characteristic properties such as the acidity of H_2SO_4.

Characteristic to the quest for understanding in this study is the seeking of similarities and differences between related systems. Here, the oxyhydroxides of Cl are taken as the complementary system. Perchloric acid finds important use as a stable and fully deprotonated electrolyte ion in aqueous solutions. Furthermore, while stable at room temperature, heat and catalysis turn $HClO_4$ into a powerful oxidant for most reduced species. The stability of oxygen bridges toward hydrolysis has a prominent role in the present effort, and indeed, there also exists an anhydrous form of perchloric acid; i.e., the Cl_2O_7 possesses a Cl−O−Cl bridge. Thus, parallel to the sulfur system, investigations of protolysis, redox, and hydrolysis (condensation) reactions in the chlorine systems can be made and consistency between the two systems sought.

A third more academic system comprises the exotic oxides of argon. Although this system has been investigated previously by means of theory, no experimental reports are available to date. The argon oxides are included here for sake of completion, but also as a challenge to the DFT description by high-level theory predictions.

Clarifying investigations into the above points of interest can quite easily be performed using quantum chemical techniques. The present work follows the principles that were outlined in two previous works on the water chemistry of some transition metal oxides.[4,5] Two types of reactions are suitable for modeling the chemical behavior of the oxides. The first type is water addition to the mononuclear species, which produces hydrates or hydroxides. The second type comprises degradation of polynuclear oxide species by hydrolytic cleavage of S−O−S and Cl−O−Cl bridges. The products of the hydrolysis reactions are mononuclear hydroxides.

As perchloric acid is unstable toward reduction, a subsection in the present study addresses this property, and comparisons to sulfuric acid and ArO_4 are made. Apart from the formation of H_2O_2 in water addition reactions, reactions including the addition of H_2 and the release of O_2 are also treated.

Results are presented for the following reactions with water, as well as some interconnecting reactions between the monomeric and dimeric systems:

$$SO_3(g) + H_2O(g) \rightarrow SO_3{\cdot}H_2O(g)$$

$$SO_3{\cdot}H_2O(g) \rightarrow SO_2(OH)_2(g)$$

$$SO_2(OH)_2(g) + H_2O(g) \rightarrow SO_2(OH)_2{\cdot}H_2O(g)$$

$$SO_2(OH)_2{\cdot}H_2O(g) \rightarrow SO(OH)_4(g)$$

$$SO(OH)_4(g) + H_2O(g) \rightarrow SO(OH)_4{\cdot}H_2O(g)$$

$$SO(OH)_4{\cdot}H_2O(g) \rightarrow S(OH)_6(g)$$

$$SO_2(OH)_2{\cdot}H_2O(g) + nH_2O(g) \rightarrow SO_2(OH)_2{\cdot}nH_2O(g) \qquad (R2)$$

$$S_2O_6(g) \rightarrow 2\ SO_3(g)$$

$$S_2O_6(g) + H_2O(g) \rightarrow S_2O_5(OH)_2(g)$$

$$S_2O_5(OH)_2(g) + H_2O(g) \rightarrow 2\ SO_2(OH)_2(g) \qquad (R3)$$

$$ClO_3(OH)(g) + H_2O(g) \rightarrow ClO_3(OH){\cdot}H_2O(g)$$

$$ClO_3(OH){\cdot}H_2O(g) \rightarrow ClO_2(OH)_3(g)$$

$$ClO_3(OH){\cdot}H_2O(g) \rightarrow ClO_2(OH){\cdot}H_2O_2(g)$$

$$ClO_3(OH){\cdot}H_2O(g) + H_2O(g) \rightarrow ClO_3(OH){\cdot}nH_2O(g) \qquad (R4)$$

$$Cl_2O_7(g) + H_2O(g) \rightarrow 2ClO_3(OH)(g) \qquad (R5)$$

$$ArO_4(g) + H_2O(g) \rightarrow ArO_3(g) + H_2O_2(g) \qquad (R6)$$

Methods and Computational Details

We have chosen to employ density functional theory (DFT) for the calculations in the present study. The B3LYP hybrid functional[6] was selected as the preferred method on basis of the results of previous studies. These comprise two studies on scandium oxides[7,8] and one on germanium oxides and hydroxides,[9] but of particular concern for the present work are the two investigations on water addition to transition metal oxides.[4,5] The computational results were in all cases in very close agreement with available experimental results. This expected success of the B3LYP hybrid density functional approach requires some comments. Experience on a vast number of systems tells of the robustness of the particular choice on mixing exchange and correlation terms for this functional. Only when ambiguity in the occupation of the Kohn−Sham orbitals exists can results be expected to become unreliable. This is because the conventional Kohn−Sham strategy is ill defined in cases where the proper electronic density description requires partial orbital occupations, as in bond forming and bond breaking regions on the ground state potential energy surface (PES). Such anticipated pathological systems are carefully avoided in our DFT investigations. While this constraint may appear troublesome, a similar warning flag is associated with the applicability of nondegenerate perturbation theories, such as Møller−Plesset second-order perturbation method (MP2), and indeed also coupled-cluster methods, such as CCSD(T), at times. As the accuracy of DFT has been demonstrated previously,[7−9] the high cost efficiency very much favors it before any explicitly correlated wave function based method. The agreement with ab initio results is repeatedly shown here by comparisons to a number of benchmark calculations using MP2.

The B3LYP calculations were performed on the S, Cl, and Ar oxides, oxyhydroxides, and hydroxides as outlined in the reactions R2−R6 and on water by employing the GAUSSIAN 98 program package.[10] Molecular structures were determined by calculating analytical Hessians and characterized by their stabilities and vibrational spectra. The choice of basis set requires some comments. The medium-sized 6-311+G(d,p) basis set (denoted by (M), used for all atoms, appears to be fully sufficient for describing the energetics and structures in general. However, the description of the S−O, Cl−O, and, in particular, Ar−O bonding can be improved significantly by selecting larger basis sets. This type of improvement turns out to be most important for S, Cl, and Ar. Thus, calculations on important structures were complemented by full optimizations using the maximal 6-311+G(3df) basis sets on S, Cl ,and Ar (denoted by (L)). This basis set extension appears to be highly

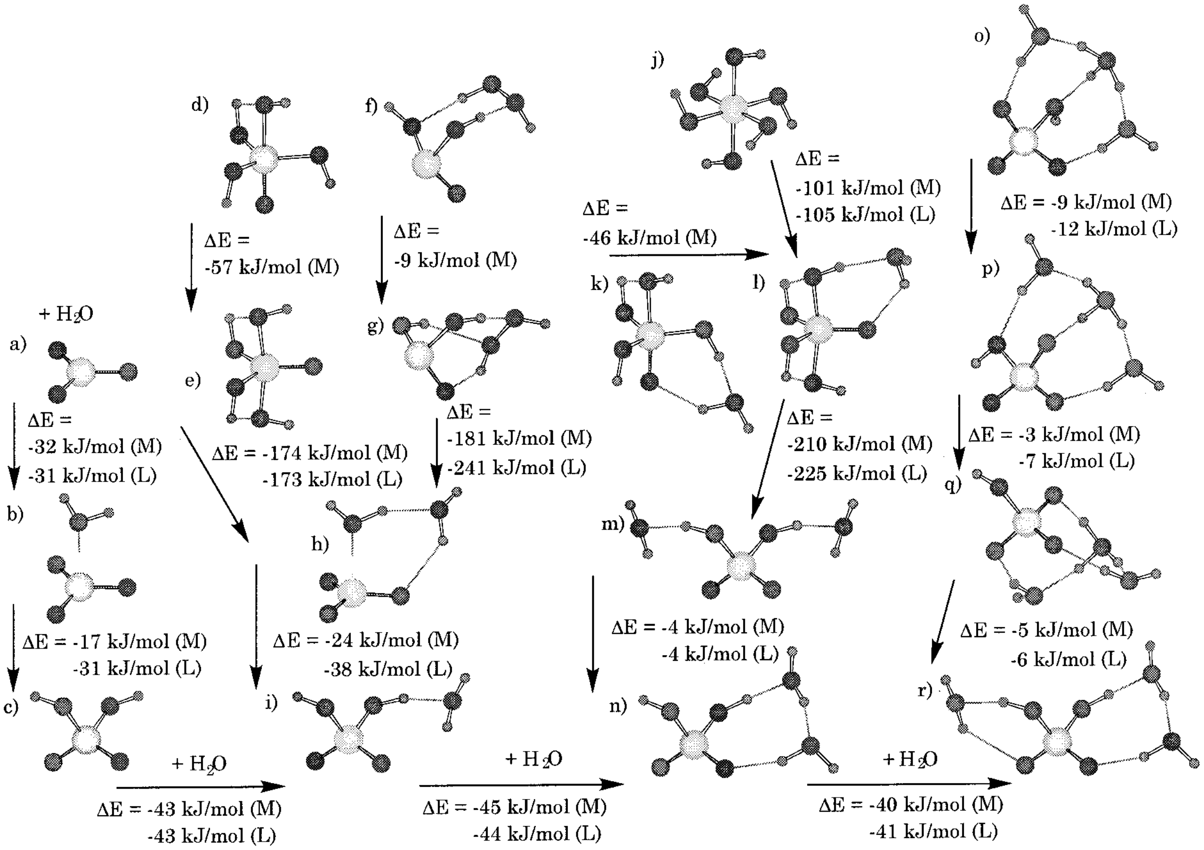

Figure 1. Structures in the $SO_3 + 4\ H_2O$ system: (a) $SO_3(g)$ (D_{3h}), (b) $SO_3{\cdot}H_2O(g)$ (C_1), (c) $SO_2(OH)_2(g)$ (C_2), (d and e) $SO(OH)_4(g)$ (C_1 and C_2), (f and g) $SO(OH)_2{\cdot}H_2O_2(g)$ (C_1), (h) $SO_3{\cdot}2\ H_2O(g)$ (C_1), (i) $SO_2(OH)_2{\cdot}H_2O(g)$ (C_1), (j) $S(OH)_6(g)$ (C_i), (k and l) $SO(OH)_4{\cdot}H_2O(g)$ (C_1), (m and n) $SO_2(OH)_2{\cdot}2\ H_2O(g)$ (C_1), (o−r) $SO_2(OH)_2{\cdot}3\ H_2O(g)$ (C_1), together with relative stabilities and energetics for some hydrolysis reactions.

efficient at a minimal extra computational cost. For O and H, 6-311+G(d,p) is sufficient for describing the bonding, which is seen in comparisons with some calculations on small S and Cl systems and on Ar oxides where the very large 6-311+G(3df,3pd) basis set was used for all atoms (denoted by (XL)). It must, however, be noted that explicitly wave function based methods, such as MP2, are much more sensitive toward an unequal basis set expansion (e.g., as in (L)), and care must be taken when analyzing such results. The smaller 6-311G basis sets for O and H atoms in conjunction with the 6-311G(d) basis sets for S and Cl were employed (denoted by (S)) for predicting structures. Although these appear reasonable, for several reactions the energetics come out wrong. This occurs when the polarization around the core molecule is altered, e.g., by deprotonation. If this effect is accounted for, the (S) basis set can be employed on large clusters to reduce computational costs further. All calculations were carried out on closed-shell singlet systems, i.e., the ground states of the investigated species in their highest oxidation state.

Results and Discussion

The present effort constitutes a systematic investigation of the stepwise addition of molecular water to the SO_3, $ClO_3(OH)$, and ArO_4 molecules, as well as to binuclear S and Cl oxide clusters. The former set of reactions is primarily designed as a measure on the reactivities of S=O, Cl=O, and Ar=O bonds toward water addition on a relative scale, following closely a similar path taken for the mononuclear transition metal oxides.[4] Issues concerning microsolvation are considered below as competition between hydrolysis and solvation is expected. A third main objective is to characterize the hydrolysis of S−O−S and Cl−O−Cl bridges. The water addition to the binuclear oxide clusters is in line with the corresponding study on transition metal oxide clusters.[5] The last subsection discusses the use of sulfuric acid and perchloric acid as oxidants and includes the water chemistry of ArO_4, both for completion and for methodological benchmarking.

The computational procedure includes full geometry optimization of all reactants and products. This is complemented by a vibrational analysis to find model structures that are local energy minima. For several of the model species, there exist more than one minimum structure within the same stoichiometry. It becomes important for the chemical understanding to characterize structures and paths as well as energy minima and to evaluate relative stabilities along the reaction coordinates. Summaries of geometrical parameters and vibrational frequencies for these structures are provided in Tables 1−5, and illustrated in Figures 1−5.

$SO_3(g) + nH_2O$. The $SO_3(g)$ molecule (Figure 1a) is planar with three equivalent S=O bonds (1.45 Å (M) and 1.43 Å (L/XL)). Exactly the same basis set effect on the bond distances is found when using MP2, and the S=O bond lengths has also been determined experimentally to 1.43 Å.[11] Thus, the (M) basis set appears insufficient for an accurate description of $SO_3(g)$. Very good agreement is also obtained with experimental IR-active frequencies (490, 527, and 1385 cm^{-1} by Givan et al.[12] vs 492−495, 522−524, and 1398−1404 cm^{-1} from B3LYP and L/XL) using DFT and large basis sets. Water addition to $SO_3(g)$ has recently been treated thoroughly in two quantum chemical studies, using B3LYP and basis sets of (M) quality.[13,14] The main conclusions drawn were that the hydrolysis of one S=O bond in $SO_3(g)$ displayed a much lower reaction barrier

TABLE 1: Summaries of Bond Lengths R (Å) and Bond Angles A (deg) and Ranges of Vibrational Frequencies (cm^{-1}), Together with Normal-Mode Symmetries and the Number of Vibrations in Each Group, for the $SO_3 + n\ H_2O$ System

SO_3				
D_{3h} (M)	R(S=O): 1.447	A(O=S=O): 120.0		$A_2'' + E'$ (2 vib.): 441−496 $A_1' + E'$ (1 + 1 vib.): 1017−1329
D_{3h} (L)	R(S=O): 1.425	A(O=S=O): 120.0		$A_2'' + E'$ (2 vib.): 492−522 $A_1' + E'$ (1+1 vib.): 1078−1404
D_{3h} (XL)	R(S=O): 1.426	A(O=S=O): 120.0		$A_2''+E'$ (2 vib.): 495−524 $A_1' + E'$ (1+1 vib.): 1075−1398
D_{3h} (MP2/M):	R(S=O): 1.449	A(O=S=O): 120.0		
D_{3h} (MP2/L):	R(S=O): 1.429	A(O=S=O): 120.0		
D_{3h} (MP2/XL):	R(S=O): 1.429	A(O=S=O): 120.0		
$SO_3 \cdot H_2O$				
C_1 (M)	R(S=O): 1.446−1.449 R(S···O): 2.415	R(O−H): 0.965 A(S···O−H): 114.5−115.0	A(O=S=O): 119.5−120.2 A(O=S···O): 92.4−94.4 A(H−O−H): 106.5	A (9 vib.): 29−533 A (4 vib.): 1021−1611 A (2 vib.): 3793−3897
C_1 (L)	R(S=O): 1.423−1.427 R(S···O): 2.374	R(O−H): 0.965 A(S···O−H): 108.7	A(O=S=O): 119.4−119.8 A(O=S···O): 92.1−95.0 A(H−O−H): 106.6	A (9 vib.): 25−560 A (4 vib.): 1080−1616 A (2 vib.): 3784−3888
C_1 (XL)	R(S=O): 1.423−1.427 R(S···O): 2.377	R(O−H): 0.964 A(S···O−H): 105.7	A(O=S=O): 119.4−119.8 A(O=S···O): 92.1−95.2 A(H−O−H): 106.3	A (9 vib.): 25−560 A (4 vib.): 1080−1616 A (2 vib.): 3784−3888
C_1 (MP2/M)	R(S=O): 1.446−1.448 R(S···O): 2.491	R(O−H): 0.962 A(S···O−H): 118.5−118.8	A(O=S=O): 119.6−120.3 A(O=S···O): 91.0−94.2 A(H−O−H): 104.8	
C_1 (MP2/L)	R(S=O): 1.425−1.428 R(S···O): 2.425	R(O−H): 0.963 A(S···O−H): 111.5−111.7	A(O=S=O): 119.6−119.9 A(O=S···O): 91.6−93.7 A(H−O−H): 105.0	
C_1 (MP2/XL)	R(S=O): 1.425−1.429 R(S···O): 2.389	R(O−H): 0.962 A(S···O−H): 105.8−106.5	A(O=S=O): 119.5−120.0 A(O=S···O): 91.5−94.3 A(H−O−H): 105.0	
$SO_2(OH)_2$				
C_2 (M)	R(S=O): 1.439 R(S−O): 1.626	R(O−H): 0.970 A(S−O−H): 109.5	A(O=S=O): 124.6 A(O=S−O): 105.3−108.9 A(O−S−O): 101.6	A + B (7 + 6 vib.): 261−1413 A + B (1 + 1 vib.): 3759−3763
C_2 (L)	R(S=O): 1.420 R(S−O): 1.593	R(O−H): 0.970 A(S−O−H): 109.4	A(O=S=O): 124.1 A(O=S−O): 105.5−108.8 A(O−S−O): 102.0	A + B (7 + 6 vib.): 266−1471 A + B (1 + 1 vib.): 3766−3771
C_2 (XL)	R(S=O): 1.420 R(S−O): 1.593	R(O−H): 0.968 A(S−O−H): 109.4	A(O=S=O): 124.0 A(O=S−O): 105.6−108.7 A(O−S−O): 102.1	A + B (7 + 6 vib.): 248−1467 A + B (1 + 1 vib.): 3765−3769
C_2 (MP2/M)	R(S=O): 1.433 R(S−O): 1.614	R(O−H): 0.968 A(S−O−H): 108.9	A(O=S=O): 124.8 A(O=S−O): 105.2−109.0 A(O−S−O): 101.4	
C_2 (MP2/L)	R(S=O): 1.418 R(S−O): 1.584	R(O−H): 0.969 A(S−O−H): 107.9	A(O=S=O): 124.1 A(O=S−O): 105.3−109.0 A(O−S−O): 102.1	
C_2 (MP2/XL)	R(S=O): 1.419 R(S−O): 1.583	R(O−H): 0.967 A(S−O−H): 108.4	A(O=S=O): 124.3 A(O=S−O): 105.3−108.8 A(O−S−O): 102.1	
$SO(OH)_4$				
C_1 (1-M)	R(S=O): 1.486 R(S−O): 1.633−1.758 R(O−H): 0.965−0.973 R(O···H): 1.904−2.145	A(S−O−H): 103.8−109.9 A(S−O···H): 68.2−71.5	A(O=S−O): 95.9−177.9 A(O−S−O): 83.0−122.9 A(O−H···O): 90.5−97.6 A(H−O···H): 164.4	A (20 vib.): 94−1334 A (4 vib.): 3692−3819
C_2 (2-M)	R(S=O): 1.469 R(S−O): 1.630−1.731 R(O−H): 0.965−0.973 R(O···H): 1.948	A(S−O−H): 105.6−107.0 A(S−O···H): 69.7	A(O=S−O): 96.5−123.4 A(O−S−O): 86.2−167.0 A(O−H···O): 98.0 A(H−O···H): 144.6	A + B (10+10 vib.): 145−1293 A + B (2+2 vib.): 3693−3821
C_2 (2-L)	R(S=O): 1.451 R(S−O): 1.600−1.703 R(O−H): 0.965−0.972 R(O···H): 1.942	A(S−O−H): 106.0−109.5 A(S−O···H): 69.5	A(O=S−O): 95.7−123.9 A(O−S−O): 86.5−168.5 A(O−H···O): 97.0 A(H−O···H): 138.5	A + B (10 + 10 vib.): 192−1314 A + B (2 + 2 vib.): 3710−3829
$SO(OH)_2 \cdot H_2O_2$				
C_1 (1-M)	R(S=O): 1.463 R(S−O): 1.632−1.730 R(O−O): 1.448 R(O−H): 0.969−0.992 R(O···H): 1.797−1.914	A(S−O−H): 109.3−109.5 A(S−O···H): 112.7 A(H−O···H): 113.8−115.3	A(O=S−O): 101.2−109.7 A(O−S−O): 97.5 A(O−H···O): 161.3−161.7 A(O−O−H): 101.3−102.2 A(O−O···H): 114.5	A (20 vib.): 58−1520 A (4 vib.): 3338−3764
C_1 (2-M)	R(S=O): 1.490 R(S−O): 1.645−1.653 R(O−O): 1.450 R(O−H): 0.967−0.987 R(O···H): 1.824−2.144	A(S−O−H): 110.4−110.5 A(S=O···H): 111.5 A(H−O···H): 83.0−138.6	A(O=S−O): 101.2−109.7 A(O−S−O): 97.5 A(O−H···O): 143.6−154.5 A(O−O−H): 96.6−102.3 A(O−O···H): 101.1−109.4	A (20 vib.): 80−1519 A (4 vib.): 3419−3782

TABLE 1 (Continued)

		$SO(OH)_2 \cdot H_2O_2$		
C_1	*R*(S═O): 1.470	*A*(S−O−H): 110.4−110.6	*A*(O═S−O): 106.0−106.3	A (20 vib.): 74−1508
(2-L)	*R*(S−O): 1.612−1.622		*A*(O−S−O): 101.2	A (4 vib.): 3416−3777
	R(O−O): 1.450	*A*(S═O···H): 111.2	*A*(O−H···O): 143.5−156.9	
	R(O−H): 0.968−0.987	*A*(H−O···H): 79.4−135.2	*A*(O−O−H): 101.0−102.3	
	R(O···H): 1.824−2.184		*A*(O−O···H): 96.8−107.9	
		$SO_3 \cdot 2H_2O$		
C_1	*R*(S═O): 1.443−1.456	*A*(S═O···H): 124.0	*A*(O═S═O): 118.5−120.0	A (14 vib.): 22−647
(M)	*R*(S···O): 2.234	*A*(S···O−H): 107.2−110.7	*A*(O═S···O): 93.5−96.5	A (6 vib.): 918−1643
	R(O−H): 0.965−0.989	*A*(H−O−H): 107.0−107.9	*A*(O−H···O): 134.3−158.4	A (4 vib.): 3368−3898
	R(O···H): 1.733−2.083	*A*(H−O···H): 98.6−131.7		
C_1	*R*(S═O): 1.422−1.434	*A*(S═O···H): 123.7	*A*(O═S═O): 118.5−119.8	A (14 vib.): 21−688
(L)	*R*(S···O): 2.166	*A*(S···O−H): 106.7−107.5	*A*(O═S···O): 94.6−96.7	A (6 vib.): 956−1656
	R(O−H): 0.962−0.992	*A*(H−O−H): 107.0−108.0	*A*(O−H···O): 131.3−161.2	A (4 vib.): 3319−3897
	R(O···H): 1.712−2.125	*A*(H−O···H): 98.8−130.7		
		$SO_2(OH)_2 \cdot H_2O$		
C_1	*R*(S═O): 1.440−1.449	*A*(S═O···H): 110.8	*A*(O═S═O): 123.0	A (19 vib.): 44−1420
(M)	*R*(S−O): 1.596−1.631	*A*(S−O−H): 109.2	*A*(O═S−O): 104.4−109.3	A (2 vib.): 1616−3202
	R(O−H): 0.962−1.000	*A*(H−O−H): 107.0	*A*(O−S−O): 102.4	A (3 vib.): 3759−3895
	R(O···H): 1.691−2.242	*A*(H−O···H): 100.6−126.8	*A*(O−H···O): 122.0−163.0	
C_1	*R*(S═O): 1.421−1.429	*A*(S═O···H): 110.9	*A*(O═S═O): 122.6	A (19 vib.): 46−1463
(M)	*R*(S−O): 1.564−1.600	*A*(S−O−H): 109.0−109.6	*A*(O═S−O): 107.5−109.2	A (2 vib.): 1617−3183
	R(O−H): 0.962−1.000	*A*(H−O−H): 107.0	*A*(O−S−O): 102.8	A (3 vib.): 3762−3894
	R(O···H): 1.676−2.264	*A*(H−O···H): 99.6−126.2	*A*(O−H···O): 121.5−164.4	
		$S(OH)_6$		
C_i	*R*(S−O): 1.702	*A*(S−O−H): 106.3	*A*(O−S−O): 88.6−180.0	$A_g + A_u$ (9+12 vib.): 178−778
(M)	*R*(O−H): 0.967			$A_g + A_u$ (3+3 vib.): 1174−1244
				$A_g + A_u$ (3+3 vib.): 3788−3793
C_i	*R*(S−O): 1.675	*A*(S−O−H): 106.3	*A*(O−S−O): 88.6−180.0	$A_g + A_u$ (9+12 vib.): 192−802
(L)	*R*(O−H): 0.967			$A_g + A_u$ (3+3 vib.): 1196−1267
				$A_g + A_u$ (3+3 vib.): 3797−3802
		$SO(OH)_4 \cdot H_2O$		
C_1	*R*(S═O): 1.502	*A*(S═O···H): 68.4−120.7	*A*(O═S−O): 94.5−176.4	A (26 vib.): 57−1434
(1-M)	*R*(S−O): 1.629−1.763	*A*(S−O−H): 103.5−109.6	*A*(O−S−O): 82.8−120.3	A (2 vib.): 1623−3171
	R(O−H): 0.962−1.000	*A*(S−O···H): 71.5	*A*(O−H···O): 91.7−167.5	A (5 vib.): 3635−3887
	R(O···H): 1.698−2.100	*A*(H−O−H): 107.3	*A*(H−O···H): 86.8−164.9	
C_1	*R*(S═O): 1.479	*A*(S═O···H): 118.8	*A*(O═S−O): 95.0−122.5	A (26 vib.): 43−1327
(2-M)	*R*(S−O): 1.630−1.744	*A*(S−O−H): 105.2−110.0	*A*(O−S−O): 85.3−166.9	A (2 vib.): 1612−3460
	R(O−H): 0.962−0.984	*A*(S−O···H): 70.0−70.4	*A*(O−H···O): 97.3−162.0	A (5 vib.): 3687−3893
	R(O···H): 1.800−2.065	*A*(H−O−H): 106.7	*A*(H−O···H): 89.2−149.8	
C_1	*R*(S═O): 1.459	*A*(S═O···H): 121.0	*A*(O═S−O): 94.4−123.0	A (26 vib.): 40−1348
(2-L)	*R*(S−O): 1.600−1.716	*A*(S−O−H): 105.7−105.9	*A*(O−S−O): 85.9−168.0	A (2 vib.): 1612−3471
	R(O−H): 0.962−0.983	*A*(S−O···H): 69.8−70.3	*A*(O−H···O): 97.6−165.0	A (5 vib.): 3705−3893
	R(O···H): 1.798−2.079	*A*(H−O−H): 106.7	*A*(H−O···H): 88.0−146.0	
		$SO_2(OH)_2 \cdot 2H_2O$		
C_2	*R*(S═O): 1.451	*A*(S═O···H): 110.6	*A*(O═S═O): 121.7	A + B (13 + 12 vib.): 32−1419
(1-M)	*R*(S−O): 1.600	*A*(S−O−H): 109.8	*A*(O═S−O): 106.3−108.8	A + B (2 + 2 vib.): 1617−3242
	R(O−H): 0.962−0.997	*A*(H−O−H): 106.9	*A*(O−S−O): 103.4	A + B (2 + 2 vib.): 3744−3892
	R(O···H): 1.711−2.187	*A*(H−O···H): 98.3−125.8	*A*(O−H···O): 125.4−161.8	
C_2	*R*(S═O): 1.431	*A*(S═O···H): 110.8	*A*(O═S═O): 121.2	A + B (13 + 12 vib.): 30−1455
(1-L)	*R*(S−O): 1.569	*A*(S−O−H): 109.5	*A*(O═S−O): 106.5−108.8	A + B (2 + 2 vib.): 1619−3232
	R(O−H): 0.962−0.997	*A*(H−O−H): 106.8	*A*(O−S−O): 103.6	A + B (2 + 2 vib.): 3747−3891
	R(O···H): 1.696−2.220	*A*(H−O···H): 97.0−125.0	*A*(O−H···O): 125.2−163.0	
C_1	*R*(S═O): 1.441−1.453	*A*(S═O···H): 138.4	*A*(O═S═O): 121.6	A (25 vib.): 36−1415
(2-M)	*R*(S−O): 1.577−1.634	*A*(S−O−H): 108.9−113.4	*A*(O═S−O): 103.8−110.5	A (4 vib.): 1630−3399
	R(O−H): 0.962−1.023	*A*(H−O−H): 106.7−107.4	*A*(O−S−O): 103.0	A (4 vib.): 3671−3888
	R(O···H): 1.550−1.892	*A*(H−O···H): 99.3−125.5	*A*(O−H···O): 156.2−177.2	
C_1	*R*(S═O): 1.422−1.432	*A*(S═O···H): 139.9	*A*(O═S═O): 121.2	A (25 vib.): 32−1449
(2-L)	*R*(S−O): 1.548−1.600	*A*(S−O−H): 108.9−113.5	*A*(O═S−O): 104.0−110.5	A (4 vib.): 1624−3402
	R(O−H): 0.962−1.023	*A*(H−O−H): 106.7−107.3	*A*(O−S−O): 103.2	A (4 vib.): 3681−3889
	R(O···H): 1.548−1.917	*A*(H−O···H): 99.4−125.4	*A*(O−H···O): 154.3−177.0	
		$SO_2(OH)_2 \cdot 3H_2O$		
C_1	*R*(S═O): 1.459−1.487	*A*(S═O···H): 126.9−131.4	*A*(O═S═O): 113.9−117.5	A (30 vib.): 47−1485
(1-M)	*R*(S−O): 1.754	*A*(S−O−H): 107.6	*A*(O═S−O): 99.9−103.6	A (9 vib.): 1640−3387
	R(O−H): 0.969−1.043	*A*(S−O···H): 113.8	*A*(O−H···O): 156.2−177.2	A (3 vib.): 3811−3883
	R(O···H): 1.515−1.722	*A*(H−O−H): 104.2−107.5	*A*(H−O···H): 101.3−125.4	
C_1	*R*(S═O): 1.431−1.457	*A*(S═O···H): 128.7−131.6	*A*(O═S═O): 113.5−117.0	A (30 vib.): 42−1485
(1-L)	*R*(S−O): 1.708	*A*(S−O−H): 107.9	*A*(O═S−O): 100.8−103.6	A (9 vib.): 1634−3373
	R(O−H): 0.962−1.040	*A*(S−O···H): 114.5	*A*(O−H···O): 159.9−165.9	A (3 vib.): 3812−3882
	R(O···H): 1.488−1.715	*A*(H−O−H): 104.4−107.9	*A*(H−O···H): 102.7−124.0	

TABLE 1 (Continued)

		$SO_2(OH)_2·3H_2O$		
C_1	*R*(S═O): 1.424−1.510	*A*(S═O···H): 116.5−129.6	*A*(O═S═O): 112.2−118.8	A (30 vib.): 51−1457
(2-M)	*R*(S−O): 1.706	*A*(S−O−H): 106.9	*A*(O═S−O): 101.4−104.9	A (9 vib.): 1640−3567
	R(O−H): 0.969−1.064	*A*(S−O···H): 117.6	*A*(O−H···O): 158.0−170.6	A (3 vib.): 3790−3881
	R(O···H): 1.453−1.856	*A*(H−O−H): 104.3−107.4	*A*(H−O···H): 99.8−123.9	
C_1	*R*(S═O): 1.428−1.475	*A*(S═O···H): 119.0−129.4	*A*(O═S═O): 112.6−116.8	A (30 vib.): 44−1450
(2-L)	*R*(S−O): 1.663	*A*(S−O−H): 108.0	*A*(O═S−O): 99.8−106.0	A (9 vib.): 1632−3605
	R(O−H): 0.962−1.063	*A*(S−O···H): 120.9	*A*(O−H···O): 159.7−170.8	A (3 vib.): 3791−3881
	R(O···H): 1.420−1.893	*A*(H−O−H): 103.0−108.9	*A*(H−O···H): 101.0−123.7	
C_1	*R*(S═O): 1.484−1.504	*A*(S═O···H): 115.2−121.3	*A*(O═S═O): 111.6−114.9	A (30 vib.): 57−1469
(3-M)	*R*(S−O): 1.635	*A*(S−O−H): 113.0	*A*(O═S−O): 103.0−106.6	A (9 vib.): 1643−3476
	R(O−H): 0.962−1.043	*A*(H−O−H): 108.0−115.3	*A*(O−H···O): 149.4−160.9	A (3 vib.): 3780−3886
	R(O···H): 1.456−1.710	*A*(H−O···H): 109.7−133.0		
C_1	*R*(S═O): 1.447−1.483	*A*(S═O···H): 113.4−120.4	*A*(O═S═O): 111.5−115.6	A (30 vib.): 53−1460
(3-L)	*R*(S−O): 1.596	*A*(S−O−H): 108.9	*A*(O═S−O): 103.6−106.9	A (9 vib.): 1637−3485
	R(O−H): 0.962−1.050	*A*(H−O−H): 103.4−108.5	*A*(O−H···O): 160.0−167.4	A (3 vib.): 3788−3886
	R(O···H): 1.469−1.805	*A*(H−O···H): 103.9−124.9		
C_1	*R*(S═O): 1.451−1.454	*A*(S═O···H): 110.0−136.8	*A*(O═S═O): 120.2	A (31 vib.): 28−1411
(4-M)	*R*(S−O): 1.582−1.603	*A*(S−O−H): 108.7−112.9	*A*(O═S−O): 105.8−110.2	A (6 vib.): 1617−3402
	R(O−H): 0.962−1.019	*A*(H−O−H): 106.7−107.0	*A*(O−S−O): 103.9	A (5 vib.): 3655−3891
	R(O···H): 1.570−2.178	*A*(H−O···H): 97.9−125.2	*A*(O−H···O): 126.3−176.8	
C_1	*R*(S═O): 1.431−1.434	*A*(S═O···H): 110.0−138.4	*A*(O═S═O): 119.9	A (31 vib.): 24−1442
(4-L)	*R*(S−O): 1.553−1.571	*A*(S−O−H): 109.0−113.0	*A*(O═S−O): 106.0−110.0	A (6 vib.): 1620−3406
	R(O−H): 0.962−1.019	*A*(H−O−H): 106.6−107.0	*A*(O−S−O): 104.0	A (5 vib.): 3663−3890
	R(O···H): 1.568−2.185	*A*(H−O···H): 96.5−125.4	*A*(O−H···O): 126.3−177.0	
		$HSO_2(OH)$		
C_1	*R*(S═O): 1.441−1.451	*R*(O−H): 0.970	*A*(O═S═O): 123.6	A (5 vib.): 212−772
(M)	*R*(S−O): 1.634	*A*(S−O−H): 109.3	*A*(O═S−O): 107.3−108.1	A (5 vib.): 1022−1380
	R(S−H): 1.363	*A*(H−S−O): 98.2	*A*(H−S═O): 108.2−108.5	A (2 vib.): 2539−3766
C_1	*R*(S═O): 1.421−1.430	*R*(O−H): 0.969	*A*(O═S═O): 123.2	A (5 vib.): 249−824
(L)	*R*(S−O): 1.600	*A*(S−O−H): 109.3	*A*(O═S−O): 107.5−108.3	A (5 vib.): 1063−1444
	R(S−H): 1.351	*A*(H−S−O): 98.2	*A*(H−S═O): 108.2−108.5	A (2 vib.): 2583−3771
		$SO(OH)_2$		
C_1	*R*(S═O): 1.460	*R*(O−H): 0.970−0.973	*A*(O═S−O): 102.5−108.6	A (7 vib.): 256−708
(1-M)	*R*(S−O): 1.667−1.686	*A*(S−O−H): 109.5−109.7	*A*(O−S−O): 98.3	A (3 vib.): 1051−1229
				A (2 vib.): 3710−3763
C_1	*R*(S═O): 1.443	*R*(O−H): 0.970−0.974	*A*(O═S−O): 102.4−107.9	A (7 vib.): 266−752
(1-L)	*R*(S−O): 1.632−1.652	*A*(S−O−H): 109.2−109.5	*A*(O−S−O): 99.0	A (7 vib.): 266−752
				A (3 vib.): 1088−1273
C_s	*R*(S═O): 1.474	*R*(O−H): 0.972	*A*(O═S−O): 106.2	A′ + A″ (4+3 vib.): 149−711
(2-M)	*R*(S−O): 1.664	*A*(S−O−H): 109.3	*A*(O−S−O): 100.6	A′ + A″ (2+1 vib.): 1044−1201
			A′ + A” (1+1 vib.): 3715−3717	
C_s	*R*(S═O): 1.456	*R*(O−H): 0.973	*A*(O═S−O): 105.8	A′ + A” (4+3 vib.): 123−755
(2-L)	*R*(S−O): 1.631	*A*(S−O−H): 109.3	*A*(O−S−O): 100.8	A′ + A″ (2+1 vib.): 1065−1241
			A′ + A” (1+1 vib.): 3707−3710	
		$SO_2·H_2O$		
C_1	*R*(S═O): 1.460	*R*(O−H): 0.963	*A*(O═S═O): 117.8	A (7 vib.): 33−510
(M)	*R*(S···O): 2.770	*A*(S···O−H): 116.4−116.9	*A*(O═S···O): 94.2−94.4	A (3 vib.): 1132−1613
			A(H−O−H): 105.8	A (2 vib.): 3807−3911
C$_1$	*R*(S═O): 1.439	*R*(O−H): 0.963	*A*(O═S═O): 118.3	A (7 vib.): 48−524
(L)	*R*(S···O): 2.767	*A*(S···O−H): 116.0−116.4	*A*(O═S···O): 94.3−94.5	A (3 vib.): 1182−1613
			A(H−O−H): 105.8	A (2 vib.): 3806−3911
		H_2S		
C_{2v}	*R*(S−H): 1.348	*A*(H−S−H): 92.5		A_1 (2 vib.): 1208−2680
(M)				B_2 (2 vib.): 2695
C_{2v}	*R*(S−H): 1.343	*A*(H−S−H): 92.5		A_1 (2 vib.): 1213−2692
(L)				B_2 (2 vib.): 2704

when the water ligand was a dimer, trimer, or tetramer, and Larson et al. found the reaction to proceed essentially with no barrier for the $SO_3·4\ H_2O(g)$ system.[14]

Typical for the $SO_3·H_2O(g)$ complex (Figure 1b) are the long S···O bond (2.42 (M), 2.37 (L), and 2.38 (XL) Å) and the lack of hydrogen bonding to any of the S═O groups. This tells of a general inertness of the S═O units in $SO_3(g)$, and additional water molecules become essential to overcoming this reluctance to react. The formation of the complex is exothermic by 32 (M), 31 (L), and 26 (XL) kJ/mol, which is coincidentally on the order of a hydrogen bond in water. This can be seen by comparing to the formation of the analogous $CrO_3·H_2O(g)$ complex from $CrO_3(g)$ and water, which is 5 times more exothermic.[4] The energetics display only small basis set effects, despite the changes in bond distances. A similarly small difference in exothermicity (33 (M), 35 (L), and 30 (XL) kJ/mol) for the complex formation is observed for MP2, despite the fact that the S···O bond distance varies significantly (2.49 (M), 2.42 (L), and 2.39 (XL) Å). This is due to the similarities in bonding when comparing reactants and products. Larson et al. found the reaction energy to be too small to overcome the energy barrier toward the formation of $SO_2(OH)_2(g)$ (Figure 1c).[14] Thus, the barrier for sulfuric acid formation lies above the $SO_3 + H_2O$ asymptote. The conversion from the complex to the acid molecule releases 17 (M), 31 (L), and 37 (XL) kJ/mol, making the total addition process exothermic by 49 (M), 62 (L), and 63 (XL) kJ/mol. The large basis set effect (13−14 kJ/mol) is attributed to the improved description of $SO_2(OH)_2(g)$ using L or XL. The basis set effects becomes even larger for MP2 calculations. While the conversion from the $SO_3{\cdot}H_2O(g)$ complex to $SO_2(OH)_2(g)$ is exothermic by 6 (M), 29 (L), and 37 (XL) kJ/mol, the total addition reaction is exothermic by 39 (M), 64 (L), and 67 (XL) kJ/mol. The latter values demonstrate the close agreement between B3LYP and MP2 energetics at the XL basis set level and that both methods produce reasonable figures, using sufficiently large basis sets. Comparing the reaction energies to the 153−165 kJ/mol obtained when water was added to $PO_2(OH)(g)$, producing $PO(OH)_3(g)$,[3] the energetics observed for the S system is significantly smaller (100 kJ/mol). Thus, $SO_3(aq)$ is a much more relevant species under wet conditions than is metaphosphoric acid, $PO_2(OH)(g)$. The $SO_2(OH)_2(g)$ global energy minimum has C_2 symmetry (OH groups in trans position), and as opposed to the $CrO_2(OH)_2(g)$ system, no cis solution is found. This is most likely a result of the shorter S−O bond distances as compared to Cr−O, in conjunction with the different oxygen coordinations, where the $SO_2(OH)_2(g)$ system is more distorted from an ideally tetrahedral configuration. This result contradicts the finding of a cis minimum by Morokuma et al. using a smaller basis set.[15] The fact that the C_{2v} structure of $SO_2(OH)_2(g)$ in the present study only displays one symmetry-breaking vibration confirms the C_2 structure as the single minimum. The S−O bond distances can be brought close to experimentally reported values by improving the basis set (1.44 and 1.63 Å (M) and 1.42 and 1.59 Å (L) vs 1.42 and 1.57 Å experimentally).[16] The experimental geometry refers to an observed C_2 structure for $SO_2(OH)_2(g)$. Benchmark calculations using MP2 produce similar structures as do B3LYP (1.43 and 1.61 Å (M), shortened to 1.42 and 1.58 Å (L/XL)). Repeatedly, this demonstrates that the 6-311+G(d,p) basis set (M) is not enough for describing highly oxidized sulfuric oxides and oxyhydroxides, independently on the choice of quantum chemical method. The calculated IR-active vibrational frequencies for $SO_2(OH)_2(g)$ closely match those determined experimentally by Givan et al.[12] (548, 558, 831, 882, 1138, 1159, 1216, and 1452 cm^{-1} vs 537−538, 550−551, 809−811, 859−862, 1146−1148, 1163−1164, 1221−1223, and 1467−1471 cm^{-1} using B3LYP and (L/XL)). The only exception is seen for the two OH stretches, which appear 200 cm^{-1} to high in the calculations.

The most stable complex produced when adding a second water molecule to form $SO_3{\cdot}2\,H_2O(g)$ is a structure containing a water dimer ligand (Figure 1h). This step releases 36 kJ/mol (M/L), which is slightly higher than that observed for the first water association. Still, both the S···OH_2 bond (2.23 (M) and 2.17 (L) Å) and the newly formed S═O···HOH bond (2.08 (M) and 2.12 (L) Å) are long. The exothermicity for the conversion to the $SO_2(OH)_2{\cdot}H_2O(g)$ complex (Figure 1i) increases somewhat (24 (M) and 38 (L) kJ/mol), as compared to the reaction involving only one water ligand. The reason for this is found in the rather substantial binding energy of H_2O to $SO_2(OH)_2(g)$, 43 kJ/mol M and L. The SO−H bond length for the OH group, which becomes hydrogen bonded to the water molecule, can be taken as a measure on hydrogen bonding. A 0.03 Å elongation is observed, i.e., 1.00 Å (M)/(L) as compared to 0.97 Å in the absence of the H bond. The tendency toward proton release is thus visible already at this stage. Still, the S═O unit is rather reluctant toward forming a hydrogen bond, displaying only a minor increase in bond distance (1.44−1.45 (M) and 1.42−1.43 (L) Å). The S═O···HOH bond is also rather long (2.24 (M) and 2.26 (L) Å). In general, the structural effects are in agreement with what was observed by Bandy et al., using a somewhat smaller basis set than L and by Morokuma et al.[15,17] Experimental spectra for hydrated $SO_2(OH)_2(g)$ has been produced by Givan et al.[12] However, they only discuss the monohydrate, despite the fact that larger complexes ought to be present (vide infra), and consequently, it becomes difficult to assign their spectra to the $SO_2(OH)_2{\cdot}H_2O(g)$ complex alone.

An alternative to the formation of this complex is the possibility to add water to one of the remaining S═O units. There are two isomers for the $SO(OH)_4(g)$ product. Both structures display trigonal bipyramid O configurations on the S atom and intramolecular hydrogen bonds. The least stable isomer (Figure 1d) has two OH groups forming a hydrogen bond, while the other two point toward the S═O unit. There are no symmetry elements in this isomer. There is a 57 kJ/mol (M) gain if all four OH groups combine into two H-bonded pairs. This isomer (Figure 1e) has C_2 symmetry, but despite the stabilization from the H bonds, it lies 174 kJ/mol (M) above the global energy minimum, $SO_2(OH)_2{\cdot}H_2O(g)$. The reason for this relative instability is found in the bonding situation on S in the five-coordinated structure. The valence orbitals on S cannot produce equivalently good covalencies in this configuration as they can in the tetrahedral structures. Evidence of this impaired bonding is the elongated S−O bond distances in $SO(OH)_4(g)$ (ranging from 1.47 to 1.76 Å), as compared to those in $SO_2(OH)_2{\cdot}H_2O(g)$ (1.44−1.63 Å).

There are two straightforward ways for adding a second water ligand to $SO_2(OH)_2{\cdot}H_2O(g)$. Addition to the second OH group in $SO_2(OH)_2$ preserves the C_2 symmetry of the core molecule, and 41 (M) and 40 kJ/mol (L) are gained when forming this complex (Figure 1m). Instead, an additional 4 kJ/mol (M)/(L) is obtained if H_2O binds to the first water ligand, thus forming a water dimer (Figure 1n). This dimer complex of $SO_2(OH)_2{\cdot}2\,H_2O(g)$ is interesting, as it shows an increased tendency toward deprotonation as compared to $SO_2(OH)_2{\cdot}H_2O(g)$. The SO−H bond length is further elongated (1.02 Å (M)/(L)), and the S═O···HOH bond is significantly shortened (1.89 (M) and 1.92 (L) Å). The effects on the S═O unit stay small (+0.01 Å).

The second water molecule can be used as ligand to any of the two structures of $SO(OH)_4(g)$ mentioned above, thus producing two types of complexes. Despite the 40 kJ/mol (M) binding energy of water to the structure in Figure 1d, the $SO(OH)_4{\cdot}H_2O(g)$ complex (Figure 1k) remains 260 kJ/mol (M) above the lowest $SO_2(OH)_2{\cdot}H_2O(g)$ structure. There is a 46 kJ/mol (M) gain when the $SO(OH)_4{\cdot}H_2O(g)$ complex in Figure 1l is formed, but it still lies 214 (M) and 229 (L) kJ/mol above the global energy minimum. Finally, adding this second H_2O molecule to the remaining S═O bond produces $S(OH)_6(g)$ (Figure 1j), though the reaction from the least stable $SO(OH)_4{\cdot}H_2O(g)$ complex is endothermic by 55 kJ/mol (M). The $S(OH)_6(g)$ molecule has inversion symmetry (C_i); i.e., all six S−O bonds are equivalent (1.71 (M) and 1.68 (L) Å). The elongation of these bonds, as compared to S−OH distances in $SO_2(OH)_2{\cdot}2\,H_2O(g)$, reflects the strained bonding situation for six-coordinated S. The unfavorable nature of the S−OH bonds is reflected in the fact that the $S(OH)_6(g)$ molecule is 315 (M) and 334 (L) kJ/mol above the $SO_2(OH)_2{\cdot}H_2O(g)$ minimum.

While it is understood from the above that only one of the S═O bonds in SO_3 is easily available for water addition, the S═O bonds are in a sense sub-optimal. One way to see this is by adding a third water ligand to $SO_2(OH)_2(g)$. When this H_2O is used to form a network of hydrogen bonds, which connects

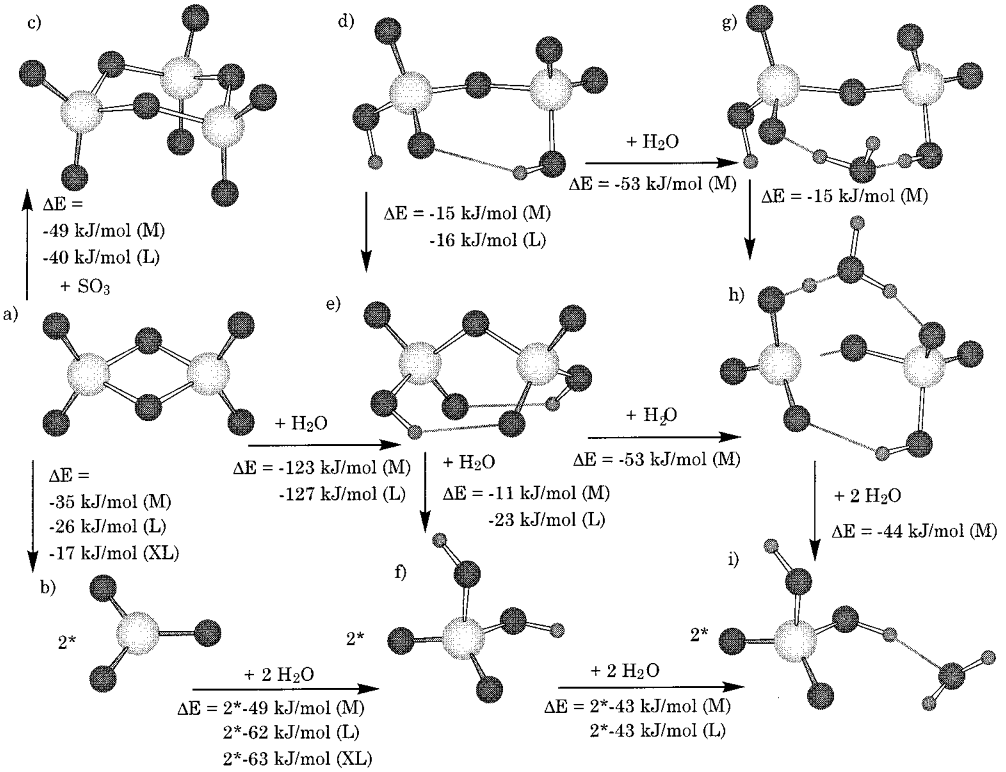

Figure 2. Structures in the $S_2O_6 + 3H_2O$ system together with S_3O_9. S_2O_6: (a) $O_2SO_2SO_2$ (D_{2h}), (b) $2SO_3$ (D_{3h}), and (c) S_3O_9 (C_{3v}). $S_2O_7H_2$: (d and e) $HO(SO_2)O(SO_2)OH$ (C_1 and C_2). $S_2O_8H_4$: (f) $2SO_2(OH)_2$ (C_2), (g and h) $HO(SO_2)O(SO_2)OH{\cdot}H_2O$ (C_1), and (i) $2SO_2(OH)_2{\cdot}H_2O$ (C_1), together with relative stabilities and energetics for some hydrolysis reactions.

three of the oxygen ligands on S, spontaneous deprotonation is observed. This nanoscale protolysis results in the formation of ion pair complexes, which consist of $HSO_4(-)/H_3O^+{\cdot}2\,H_2O(g)$. Three types of such complexes have been determined in the present study (Figure 1o–q). These complexes differ in what ligands on $SO_3(OH)(-)$ take part in the hydrogen bonding to the solvated hydronium ion. Important factors for the stability of the complexes are the microsolvation of the proton and the triple O···H bonding to the anion. While the complexes in Figure 1o,p involve hydrogen bonds to the remaining S–OH unit, the most stable ion pair has H bonds only to the S═O units (Figure 1q). The energy separation becomes 9 (M) and 12 (L) kJ/mol and 3 (M) and 7 (L) kJ/mol, respectively. The lower stability of the former two complexes can be attributed to the elongated S–OH bond (1.71–1.75 (M) and 1.66–1.71 (L) Å). The complex in Figure 1q still has this bond distance very close to that in $SO_2(OH)_2(g)$ (1.64 (M) and 1.60 (L) Åin the water complex). The S═O bond distances are somewhat elongated as compared to that of the uncoordinated acid (1.48–1.50 (M) and 1.45–1.48 (L) Å in the Figure 1q structure), and it can be noted that the proton still is in an activated position as indicated by the bond distances (SO···H, 1.47 Å; H_2O–H, 1.05 Å (L)). This fact tells that the solvation of the hydronium ion is not complete. Another indicator on the incompleteness of the $SO_2(OH)_2(g)$ solvation is that the global energy minimum for $SO_2(OH)_2{\cdot}3\,H_2O(g)$ is the complex in Figure 1r. This structure, with one H_2O monomer and one H_2O dimer ligand, still has both protons bonded to the sulfuric acid core. However, both SO–H bond lengths are elongated as compared with those of $SO_2(OH)_2(g)$, and as has been shown both by Bandy et al. and Morokuma et el., further water ligands will produce the solvated ion pair as the only structure.[15,17] The energy separation between the structures in Figure 1q,r is small (5 (M) and 6 (L) kJ/mol), which tells that both complexes are relevant for describing the microsolvation of sulfuric acid. The total energy gain by adding water to form the complex in Figure 1r is 40 (M) and 41 (L) kJ/mol. These values (40–45 kJ/mol) appear to be characteristic for addition of one $H_2O(g)$ to sulfuric acid.

The proton transfer in the $HSO_4(-)/H_3O^+{\cdot}2\,H_2O$ ion pair is a consequence of the nonoptimal bonding in the S═O units, in conjunction with the strive to level out the broken symmetry in $SO_2(OH)_2(g)$, i.e., between S═O and S–OH. An efficient way to distribute the bond strain in the S═O unit over several O atoms implies the gradual delocalization of the proton over these oxygens. The degree of deprotonation can be can be controlled in detail by the polarization of the H_2O that connect the O atoms on S. It is not unexpected to find that water complexes of strong acids produce ion pairs, but it is conceptually satisfactory be able to determine the degree to which this is a local property on the nanoscale. Obviously, a consequence of the polar complex formed, i.e., hydronium and anion, is that this system is susceptible to dissolution in water, making sulfuric acid a strong Brønsted acid.

$S_2O_6(g) + nH_2O$. The $O_2{>}S{<}O_2{>}S{<}O_2$ cluster (Figure 2a) constitutes the dimer of the $SO_3(g)$ molecule (Figure 2b). It is a natural starting point for investigating on the stabilities of S–O–S bridges. The strained bonding in the central S_2O_2 ring of $S_2O_6(g)$ cluster acts to destabilize the structure, despite the reduced number of S═O groups. The relative stability of monomers versus dimer is related to the rather low exothermicity for hydrolysis of an S═O bond in the monomer (vide supra). The splitting of the $S_2O_6(g)$ cluster into two $SO_3(g)$ fragments is exothermic by 35 (M), 26 (L), and 17 (XL) kJ/mol. The basis set effect is caused by the decreased stability of the S═O units in $SO_3(g)$ when the (L) or (XL) basis sets are used. The $CrO_3(g)$ and $Cr_2O_6(g)$ systems comprise a suitable reference. Thus, exothermicity upon hydrolysis on CrO_3 was found to be significantly greater, and consistently, the binuclear system was

TABLE 2: Summaries of Bond Lengths *R* (Å) and Bond Angles *A* (deg) and Ranges of Vibrational Frequencies (cm^{-1}), Together with Normal-Mode Symmetries and the Number of Vibrations in Each Group, for the $(SO_3)_2 + nH_2O$ Systems

		$O_2SO_2SO_2$		
D_{2h}	*R*(S═O): 1.431	*A*(O−S−O): 84.2	*A*(S−O−S): 95.8	$A_{g/u} + B_{1g/u} + B_{2g/u} + B_{3g/u}$ (5+4+5+4 vib.): 78−1426
(M)	*R*(S−O): 1.695	*A*(O═S−O): 110.3	*A*(O═S═O): 124.4	
D_{2h}	*R*(S═O): 1.412	*A*(O−S−O): 84.7	*A*(S−O−S): 95.3	$A_{g/u} + B_{1g/u} + B_{2g/u} + B_{3g/u}$ (5+4+5+4 vib.): 91−1492
(L)	*R*(S−O): 1.654	*A*(O═S−O): 110.4	*A*(O═S═O): 123.7	
D_{2h}	*R*(S═O): 1.412	*A*(O−S−O): 84.7	*A*(S−O−S): 95.3	$A_{g/u} + B_{1g/u} + B_{2g/u} + B_{3g/u}$ (5+4+5+4 vib.): 90−1486
(XL)	*R*(S−O): 1.654	*A*(O═S−O): 110.4	*A*(O═S═O): 123.7	
		S_3O_9		
C_{3v}	*R*(S═O): 1.426−1.430	*A*(O−S−O): 97.5	*A*(S−O−S): 124.3	A (30 vib.): 94−1460
(M)	*R*(S−O): 1.676	*A*(O═S−O): 104.9−110.1	*A*(O═S═O): 125.8	
C_{3v}	*R*(S═O): 1.407−1.410	*A*(O−S−O): 97.8	*A*(S−O−S): 124.1	A (30 vib.): 99−1527
(L)	*R*(S−O): 1.639	*A*(O═S−O): 105.0−110.1	*A*(O═S═O): 125.3	
		$(HO)O_2SOSO_2(OH)$		
C_1	*R*(S═O): 1.428−1.454	*A*(S−O−H): 109.6−111.2	*A*(S−O−S): 122.0	A (25 vib.): 61−1429
(1-M)	*R*(S−O): 1.594−1.707	*A*(S−O···H): 111.3	*A*(O═S═O): 123.0−124.9	A (2 vib.): 3619−3744
	R(O−H): 0.971−0.979	*A*(O−H···O): 129.6	*A*(O═S−O): 103.5−110.8	
	R(O···H): 2.089		*A*(O−S−O): 96.9−100.3	
C_1	*R*(S═O): 1.409−1.432	*A*(S−O−H): 109.5−110.9	*A*(S−O−S): 121.8	A (25 vib.): 62−1493
(1-L)	*R*(S−O): 1.571−1.666	*A*(S−O···H): 110.5	*A*(O═S═O): 122.8−124.5	A (2 vib.): 3646−3753
	R(O−H): 0.971−0.977	*A*(O−H···O): 126.9	*A*(O═S−O): 103.6−110.7	
	R(O···H): 2.112		*A*(O−S−O): 97.5−100.6	
C_2	*R*(S═O): 1.426−1.453	*A*(S−O−H): 109.9	*A*(S−O−S): 118.9	A + B (13+12 vib.): 101−1430
(2-M)	*R*(S−O): 1.594−1.683	*A*(S−O···H): 111.2	*A*(O═S═O): 123.6	A + B (1+1 vib.): 3584−3594
	R(O−H): 0.980	*A*(O−H···O): 134.0	*A*(O═S−O): 105.3−110.4	
	R(O···H): 2.058		*A*(O−S−O): 101.5	
C_2	*R*(S═O): 1.408−1.432	*A*(S−O−H): 109.8	*A*(S−O−S): 119.5	A + B (13+12 vib.): 100−1488
(2-L)	*R*(S−O): 1.562−1.647	*A*(S−O···H): 110.6	*A*(O═S═O): 123.0	A + B (1+1 vib.): 3593−3603
	R(O−H): 0.980	*A*(O−H···O): 132.9	*A*(O═S−O): 105.8−110.4	
	R(O···H): 2.050		*A*(O−S−O): 101.7	
		$(HO)O_2SOSO_2(OH) \cdot H_2O$		
C_1	*R*(S═O): 1.430−1.456	*A*(S−O−H): 110.7−112.6	*A*(S−O−S): 125.0	A (31 vib.): 44−1628
(1-M)	*R*(S−O): 1.567−1.734	*A*(S═O···H): 139.3	*A*(O═S═O): 121.8−124.3	A (5 vib.): 2677−3869
	R(O−H): 0.971−1.029	*A*(H−O−H): 107.0	*A*(O═S−O): 101.5−111.3	
	R(O···H): 1.533−1.950	*A*(H−O···H): 102.7−117.3	*A*(O−S−O): 96.6−101.0	
			A(O−H···O): 142.6−174.5	
C_1	*R*(S═O): 1.430−1.469	*A*(S−O−H): 108.7−119.8	*A*(S−O−S): 123.7	A (31 vib.): 43−1612
(2-M)	*R*(S−O): 1.516−1.777	*A*(S═O···H): 137.0	*A*(O═S═O): 119.8−121.3	A (5 vib.): 2610−3877
	R(O−H): 0.968−1.186	*A*(H−O−H): 108.0	*A*(O═S−O): 102.8−112.7	
	R(O···H): 1.218−1.940	*A*(H−O···H): 101.5−110.5	*A*(O−S−O): 101.3−103.0	
			A(O−H···O): 138.3−173.4	

favored as compared to the monomers.[5] No experimental or theoretical data on S_2O_6(g) are known to us, but the mono- and dianions have been investigated by McKee.[18] However, these structures contain only one S−O−S bridge or an S−S linkage. This is in agreement with a D_{2h} structure for the neutral S_2O_6(g), as one of the S−O−S bridges is broken and symmetry-lowered when an electron is added. This is a direct consequence of the instability of S_2O_6(g) toward fragmentation into two SO_3(g). Consequently, Givan et al. only observe a weakly bonded SO_3(g) dimer in their matrix isolation studies.[12]

The S_2O_6(g) is also reactive toward adding further SO_3(g) molecules. In the first step, an S_3O_9(g) ring of C_{3v} symmetry is formed (Figure 2c). The S−O bond distances are 1.68 (M) and 1.64 (L) Å, which is shorter than that for S_2O_6(g), while the S═O bonds are of equal length (1.43 (M) and 1.41 (L) Å). This molecule has been postulated from some experimental studies.[12] Its formation from S_2O_6(g) and SO_3(g) is exothermic by 49 (M) and 40 (L) kJ/mol, and consequently, the formation of S_3O_9(g) from three SO_3(g) becomes exothermic by 14 kJ/mol (M/L). However, this path competes poorly with the much more exothermic hydrolysis reactions, and thus, S_3O_9(g) formation is expected only under water-free conditions.

Hydrolysis of one of the S−O−S bridges in S_2O_6(g) produces the sulfuric acid dimer, (HO)O_2S−O−SO_2(OH). There are two stable structures for this dimer, depending on relative orientation of ligands on each SO_4 unit. These can be distinguished from each other by the number of intramolecular hydrogen bonds. The structure in Figure 2d has one long H-bond (2.09 (M) and 2.11 (L) Å), which removes all symmetry elements in this molecule. It is noteworthy that the asymmetry is also displayed in the S−O−S bridge, which has a 122° bond angle typical for sp^2 hybridization on O but two different S−O bond distances (1.66−1.71 (M) and 1.63−1.67 (L) Å). Rotation of one SO_4 unit produces the structure in Figure 2e, which has two long H-bonds (2.05−2.06 Å) and lies 15 kJ/mol (M) and 16 kJ/mol (L) below the previous $S_2O_7H_2$(g) structure. Apparently, the symmetry in the H-bonds allows for the bonds in the S−O−S bridge (bond angle 119−120°) to become symmetrical (1.68 (M) and 1.65 (L) Å). The overall symmetry is C_2, which tells that there are two rotational enantiomers. The same symmetry assignment was made for $S_2O_7H_2$(s) by Hönle,[19] although the replacement of the weak intramolecular H-bonds by stronger intermolecular H-bonds affects the S−O bond distances. Still, the geometrical parameters are in general agreement with those obtained from calculations. When the structure in Figure 2d is formed by hydrolysis of S_2O_6(g), 123 (M) and 127 (L) kJ/mol are released. This exothermicity is quite similar to what was observed for the Cr systems.[5] Insofar as the terminal OH

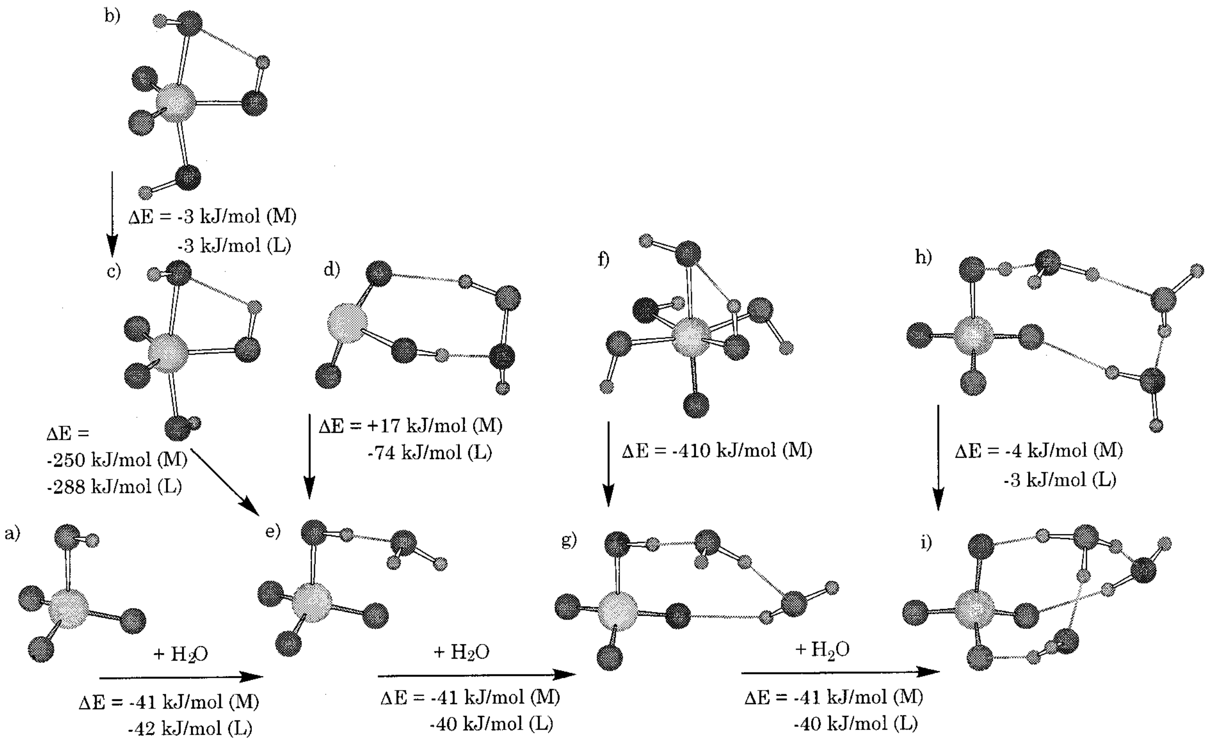

Figure 3. Structures in the $ClO_3(OH) + 3H_2O$ system: (a) $ClO_3(OH)(g)$ (C_s), (b and c) $ClO_2(OH)_3(g)$ (C_1), (d) $ClO_2(OH)\cdot H_2O_2(g)$ (C_1), (e) $ClO_3(OH)\cdot H_2O(g)$ (C_1), (f) $ClO(OH)_5(g)$ (C_1), (g) $ClO_3(OH)\cdot 2H_2O(g)$ (C_1), and (h and i) $ClO_3(OH)\cdot 3H_2O(g)$ (C_1), together with relative stabilities and energetics for some hydrolysis reactions.

groups in $HO-(O_2S)-O-(SO_2)-OH$ are regarded as truncations to a polymeric chain, the SO_3 polymers that make concentrated sulfuric acid to a highly viscous liquid can be envisaged.

Addition of a further water molecule to the remaining S−O−S bridge produces two $SO_2(OH)_2(g)$ molecules (Figure 2f). Opposite to the endothermicity (10 kJ/mol) observed for cleavage of the Cr−O−Cr bridge,[5] hydrolysis of the S analogue is exothermic by 11 (M) and 23 (L) kJ/mol. Thus, the sulfuric acid polymers are sensitive to dilution, although the energetics is rather small. An alternative to the role of H_2O as a cutting tool is the use of water as a ligand to the dimer structures. The energy gained when forming these structures is somewhat higher (53 kJ/mol (M)) than the 40−45 kJ/mol obtained when water is coordinated to the monomer. Consequently, the two $(HO)O_2SOSO_2(OH)\cdot H_2O$ structures (Figure 2g,h) appear 27 and 42 kJ/mol (M) below the asymptote of two free $SO_2(OH)_2(g)$ molecules. However, it can be argued that this energy difference is compensated by the dimerization energy of $SO_2(OH)_2(g)$. This energy has been calculated by Ianni et al. and was found to be 55 kJ/mol.[20] The fact that this value principally equals the energy gain from water adsorption on $(HO)O_2SOSO_2(OH)$ tells that hydrolysis of the chain will remain slightly exothermic. This supports an understanding that an excess of water will allow the monomeric forms to dominate. It can also be noted, that the S−O−S bridges in $(HO)O_2SOSO_2(OH)\cdot H_2O$ display a significant difference between the two S−O bond lengths. The fact that one bond is very much elongated (1.73−1.78 Å (M)) can be understood as a step toward hydrolysis of the bridge. Hydrolysis would then occur when the number of solvating water molecules becomes large enough. However, polymerization and condensation of sulfuric acid remains an important factor under dry conditions.

$ClO_3(OH)(g) + nH_2O$. The perchloric acid molecule, $ClO_3(OH)(g)$ (Figure 3a) is analogous to the $MnO_3(OH)(g)$ molecule, and both systems display C_s symmetry.[4] However, the two molecules differ significantly in the O−M−O bond angles. While permanganic acid has a nearly tetrahedral configuration of oxygens around Mn, the bond angles in the perchloric system are quite distorted from this ideal arrangement, i.e., *A*(O−Cl−O) = 101°−115° (M/L/XL). This deviation from the ideal situation reflects the difficulty for a 3p element to form a covalent bond to an X−OH unit, in conjunction with bonds to other X−OH or X=O groups. This is less of a problem for the valence orbitals of a 3d element, such as Mn. Still, both molecules are renown for their highly oxidative powers, which is due to the high oxidation state, as reflected in the three Mn=O and Cl=O groups. Regarding the structural details, the importance of a sufficiently large basis set is repeatedly underlined. Both the Cl=O and Cl−OH bond distances are shortened significantly when the size of the basis set is increased (Cl=O, 1.45−1.46 (M) vs 1.41−1.42 (L/XL) Å; Cl−OH, 1.73(M) versus 1.66 (L/XL) Å). It is gratifying to see how close these distances come to experimentally determined values (Cl=O, 1.40−1.41 Å; Cl−OH, 1.64 Å).[21] The largest remaining deviation is seen for the Cl−OH bond, but not even when the very large (XL) basis set was used could this distance be shortened. Still, the agreement is much improved as compared to a very recent study by Tao et al., where the medium-sized 6-311++G(d,p) basis set was deemed sufficient, despite that a 0.09 Å deviation remained for this bond using B3LYP.[22] It is concluded that the present description is more accurate than the calculations by these authors when employing MP2 in conjunction with this basis set.

The Cl−OH unit is the only site that is available for hydrogen bonding to a water molecule. There are gains of 41 (M) and 42 (L) kJ/mol when the $ClO_3(OH)\cdot H_2O(g)$ complex (Figure 3e) is formed, despite the fact that no hydrogen bond is formed between the water ligand and the Cl=O unit (O···H bond distance, 3.10 Å (L)). The binding energy comes solely from

TABLE 3: Summaries of Bond Lengths *R* (Å) and Bond Angles *A* (deg) and Ranges of Vibrational Frequencies (cm^{-1}), Together with Normal-Mode Symmetries and the Number of Vibrations in Each Group, for the $ClO_3(OH) + nH_2O$ System

		$ClO_3(OH)$		
C_s	*R*(Cl═O): 1.448−1.460	*R*(O−H): 0.974	*A*(O═Cl═O): 113.7−115.2	A′ + A” (7+4 vib.): 175−1231
(M)	*R*(Cl−O): 1.726	*A*(Cl−O−H): 105.5	*A*(O═Cl−O): 100.6−105.0	A′ (1 vib.): 3712
C_s	*R*(Cl═O): 1.411−1.422	*R*(O−H): 0.974	*A*(O═Cl═O): 113.6−115.1	A′ + A” (7+4 vib.): 205−1325
(L)	*R*(Cl−O): 1.662	*A*(Cl−O−H): 105.6	*A*(O═Cl−O): 100.9−105.1	A′ (1 vib.): 3715
C_s	*R*(Cl═O): 1.411−1.420	*R*(O−H): 0.972	*A*(O═Cl═O): 113.6−115.0	A′ + A” (7+4 vib.): 192−1327
(XL)	*R*(Cl−O): 1.657	*A*(Cl−O−H): 105.9	*A*(O═Cl−O): 100.9−105.1	A′ (1 vib.): 3715
		$ClO_2(OH)_3$		
C_1	*R*(Cl═O): 1.472−1.490	*A*(Cl−O−H): 99.2−104.6	*A*(O═Cl═O): 121.7	A (18 vib.): 112−1302
(1-M)	*R*(Cl−O): 1.731−1.887	*A*(Cl−O···H): 69.9	*A*(O═Cl−O): 92.4−120.7	A (3 vib.): 3555−3785
	R(O−H): 0.969−0.982	*A*(H−O···H): 139.5	*A*(O−Cl−O): 80.6−161.3	
	R(O···H): 1.816	*A*(O−H···O): 110.2		
C_1	*R*(Cl═O): 1.433−1.446	*A*(Cl−O−H): 100.0−103.9	*A*(O═Cl═O): 121.9	A (18 vib.): 95−1360
(1-L)	*R*(Cl−O): 1.663−1.852	*A*(Cl−O···H): 69.5	*A*(O═Cl−O): 92.7−117.9	A (3 vib.): 3550−3799
	R(O−H): 0.967−0.982	*A*(H−O···H): 135.0	*A*(O−Cl−O): 81.0−162.6	
	R(O···H): 1.786	*A*(O−H···O): 108.8		
C_1	*R*(Cl═O): 1.472−1.477	*A*(Cl−O−H): 100.3−105.0	*A*(O═Cl═O): 124.5	A (18 vib.): 162−1243
(2-M)	*R*(Cl−O): 1.757−1.891	*A*(Cl−O···H): 70.6	*A*(O═Cl−O): 93.0−114.3	A (3 vib.): 3569−3784
	R(O−H): 0.969−0.982	*A*(H−O···H): 137.7	*A*(O−Cl−O): 80.3−164.0	
	R(O···H): 1.848	*A*(O−H···O): 108.8		
C_1	*R*(Cl═O): 1.434−1.436	*A*(Cl−O−H): 100.4−105.0	*A*(O═Cl═O): 125.4	A (18 vib.): 179−1316
(2-L)	*R*(Cl−O): 1.683−1.854	*A*(Cl−O···H): 69.7	*A*(O═Cl−O): 92.0−114.8	A (3 vib.): 3548−3797
	R(O−H): 0.967−0.982	*A*(H−O···H): 130.2	*A*(O−Cl−O): 81.7−166.3	
	R(O···H): 1.814	*A*(O−H···O): 108.2		
		$ClO_2(OH){\cdot}H_2O_2$		
C_1	*R*(Cl═O): 1.484−1.503	*A*(Cl−O−H): 103.9	*A*(O═Cl═O): 112.5	A (18 vib.): 51−1509
(M)	*R*(Cl−O): 1.737	*A*(Cl−O···H): 121.4	*A*(O═Cl−O):104.0−106.4	A (3 vib.): 3332−3766
	R(O−O): 1.448	*A*(H−O···H): 122.5	*A*(O−O−H): 100.9−102.3	
	R(O−H): 0.968−0.994	*A*(O−H···O): 157.8−165.5	*A*(O−O···H): 115.4	
	R(O···H): 1.789−1.923			
C_1	*R*(Cl═O): 1.446−1.465	*A*(Cl−O−H): 105.4	*A*(O═Cl═O): 112.0	A (18 vib.): 41−1496
(L)	*R*(Cl−O): 1.667	*A*(Cl−O···H): 122.7	*A*(O═Cl−O):104.0−105.9	A (3 vib.): 3260−3766
	R(O−O): 1.448	*A*(H−O···H): 121.2	*A*(O−O−H): 101.0−102.2	
	R(O−H): 0.968−0.997	*A*(O−H···O): 158.0−171.5	*A*(O−O···H): 113.5	
	R(O···H): 1.752−1.964			
		$ClO_3(OH){\cdot}H_2O$		
C_1	*R*(Cl═O): 1.450−1.470	*A*(Cl−O−H): 104.6	*A*(O═Cl═O): 112.8−114.6	A (16 vib.): 35−1137
(M)	*R*(Cl−O): 1.684	*A*(H−O−H): 106.7	*A*(O═Cl−O): 102.3−106.0	A (3 vib.): 1403−3173
	R(O−H): 0.963−1.002	*A*(H−O···H): 110.0−122.6	*A*(O−H···O): 169.2	A (2 vib.): 3798−3900
	R(O···H): 1.682			
C_1	*R*(Cl═O): 1.414−1.428	*A*(Cl−O−H): 103.2	*A*(O═Cl═O): 112.8−114.5	A (16 vib.): 20−1261
(L)	*R*(Cl−O): 1.622	*A*(H−O−H): 106.5	*A*(O═Cl−O): 102.3−105.9	A (3 vib.): 1421−3157
	R(O−H): 0.964−1.003	*A*(H−O···H): 113.5−118.9	*A*(O−H···O): 175.4	A (2 vib.): 3804−3902
	R(O···H): 1.665			
		$ClO(OH)_5$		
C_1	*R*(Cl═O): 1.509	*A*(Cl−O−H): 101.0−103.3	*A*(O═Cl−O): 93.6−176.9	A (25 vib.): 123−1255
(M)	*R*(Cl−O): 1.776−1.848	*A*(Cl−O···H): 70.0	*A*(O−Cl−O): 83.5−168.9	A (5 vib.): 3698−3748
	R(O−H): 0.972−0.974	*A*(H−O···H): 141.9		
	R(O···H): 1.998	*A*(O−H···O): 102.9		
		$ClO_3(OH){\cdot}2H_2O$		
C_1	*R*(Cl═O): 1.450−1.479	*A*(Cl−O−H): 107.3	*A*(O═Cl═O): 112.0−114.9	A (23 vib.): 38−1451
(M)	*R*(Cl−O): 1.657	*A*(Cl═O···H): 128.0	*A*(O═Cl−O): 102.9−106.6	A (4 vib.): 1627−343
	R(O−H): 0.962−1.031	*A*(H−O−H): 107.4−118.0	*A*(H−O···H): 103.0−126.2	A (3 vib.): 3735−3891
	R(O···H): 1.536−2.021		*A*(O−H···O): 152.5−176.5	
C_1	*R*(Cl═O): 1.413−1.438	*A*(Cl−O−H): 107.8	*A*(O═Cl═O): 112.0−114.7	A (23 vib.): 33−1467
(L)	*R*(Cl−O): 1.597	*A*(Cl═O···H): 128.6	*A*(O═Cl−O): 103.0−106.2	A (4 vib.): 1622−3439
	R(O−H): 0.962−1.033	*A*(H−O−H): 107.4−117.6	*A*(H−O···H): 103.7−126.0	A (3 vib.): 3747−3892
	R(O···H): 1.526−2.076		*A*(O−H···O): 148.7−176.7	
		$ClO_3(OH){\cdot}3H_2O$		
C_1	*R*(Cl═O): 1.451−1.480	*A*(Cl−O−H): 109.0	*A*(O═Cl═O): 112.0−114.8	A (29 vib.): 30−1425
(1-M)	*R*(Cl−O): 1.642	*A*(Cl═O···H): 133.3	*A*(O═Cl−O): 103.4−106.7	A (6 vib.): 1633−3470
	R(O−H): 0.962−1.051	*A*(H−O−H): 106.3−107.5	*A*(H−O···H): 110.4−124.7	A (4 vib.): 3712−3888
	R(O···H): 1.461−1.920		*A*(O−H···O): 168.4−175.0	
C_1	*R*(Cl═O): 1.414−1.440	*A*(Cl−O−H): 109.5	*A*(O═Cl═O): 111.8−114.6	A (29 vib.): 22−1444
(1-L)	*R*(Cl−O): 1.582	*A*(Cl═O···H): 129.5	*A*(O═Cl−O): 103.7−106.7	A (6 vib.): 1626−3467
	R(O−H): 0.962−1.053	*A*(H−O−H): 106.4−107.3	*A*(H−O···H): 111.7−124.0	A (4 vib.): 3718−3889
	R(O···H): 1.452−1.957		*A*(O−H···O): 165.2−175.2	
C_1	*R*(Cl═O): 1.458−1.536	*A*(Cl═O···H): 115.8−125.0	*A*(O═Cl═O): 107.8−111.3	A (28 vib.): 43−1464
(2-M)	*R*(O−H): 0.962−1.027	*A*(H−O−H): 104.0−108.5	*A*(H−O···H): 103.8−124.0	A (9 vib.): 1638−3551
	R(O···H): 1.545−1.833		*A*(O−H···O): 159.3−163.5	A (2 vib.): 3878−3879

TABLE 3 (Continued)

$ClO_3(OH)\cdot 3H_2O$				
C_1	*R*(Cl═O): 1.421−1.491	*A*(Cl═O···H): 115.3−126.0	*A*(O═Cl═O): 108.0−111.2	A (28 vib.): 43−1464
(2-L)	*R*(O−H): 0.962−1.030		*A*(H−O···H): 103.4−124.4	A (9 vib.): 1638−3551
	R(O···H): 1.530−1.852	*A*(H−O−H): 104.0−109.0	*A*(O−H···O): 157.5−163.4	A (2 vib.): 3878−3879
$HClO_3$				
C_{3v}	*R*(Cl═O): 1.462	*A*(H−Cl═O): 103.8	*A*(O═Cl═O): 114.5	A_1 + E (2+3 vib.): 460−1139
(M)	*R*(Cl−H): 1.354			A_1 (1 vib.): 2373
C_{3v}	*R*(Cl═O): 1.423	*A*(H−Cl═O): 103.8	*A*(O═Cl═O): 114.5	A_1 + E (2+3 vib.): 510−1263
(L)	*R*(Cl−H): 1.332			A_1 (1 vib.): 2479
$ClO_2(OH)$				
C_s	*R*(Cl═O): 1.483	*R*(O−H): 0.975	*A*(O═Cl═O): 113.4	A′ + A” (5+3 vib.): 132−1113
(M)	*R*(Cl−O): 1.794	*A*(Cl−O−H): 104.6	*A*(O═Cl−O): 105.0	A′ (1 vib.): 3701
C_1	*R*(Cl═O): 1.435−1.448	*R*(O−H): 0.972	*A*(O═Cl═O): 114.9	A (8 vib.): 128−1235
(L)	*R*(Cl−O): 1.737	*A*(Cl−O−H): 104.7	*A*(O═Cl−O): 100.7−103.1	A (1 vib.): 3736
HCl				
$C_{\infty v}$ (M)	*R*(Cl−H): 1.287			sg (1 vib.): 2925
$C_{\infty v}$ (L)	*R*(Cl−H): 1.281			sg (1 vib.): 2946
$C_{\infty v}$ (XL)	*R*(Cl−H): 1.281			sg (1 vib.): 2945
ClO_4^-				
T_d (M)	*R*(Cl═O): 1.501	*A*(O═Cl═O): 109.5		A_1 + E + T_2 (1+1+2 vib.): 397−969
T_d (XL)	*R*(Cl═O): 1.457	*A*(O═Cl═O): 109.5		A1 + E + T2 (1+1+2 vib.): 446−1093

the formation of a hydrogen bond between the water ligand and the proton in the Cl−OH group. Consequently, the ClO−H bond distance is elongated from 0.97 to 1.00 Å, while the Cl−OH bond is shortened from 1.66 to 1.62 Å (L). If the water ligand reacts with one of the Cl═O units, the $ClO_2(OH)_3(g)$ molecule is formed (Figure 3b,c). This species contains a distorted trigonal bipyramid of O atoms surrounding the central Cl atom, and there are two isomers differing in the orientation of one of the Cl−OH groups. Symptomatic to both structures (energy separation 3 kJ/mol) are the elongated Cl−O bonds, which are indicators on the problematic bonding situation. The most stable structure for $ClO_2(OH)_3(g)$ lies 250 (M) and 288 (L) kJ/mol above the $ClO_3(OH)\cdot H_2O(g)$ complex, and this type of addition reaction is consequently unlikely to occur.

Adding a second water molecule to the $ClO_3(OH)\cdot H_2O(g)$ complex produces a structure with a water dimer ligand (Figure 3g). The energy gain upon the addition is 41 (M) and 40 (L) kJ/mol, which is very close to what was observed for the first addition step. In this complex, the ClO−H bond distance is further elongated (1.03 Å), while the Cl−OH bond is shortened to 1.60 Å (L). A long hydrogen bond to the Cl═O group is formed (2.08 Å (L)), but the water bridge still is unable to deprotonate the acid. However, deprotonation occurs readily for $ClO_3(OH)\cdot 2\ H_2O(g)$ when the small (S) basis set is used. This is an erroneous the result of too simple a description of both perchloric acid and water. In particular, the H bonds to the Cl═O unit come out far too short and strong. Reaction between a water molecule and one of the Cl═O units in $ClO_2(OH)_3(g)$ produces the six-coordinated $ClO(OH)_5(g)$ molecule (Figure 3f). This species displays en even more problematic bonding situation than $ClO_2(OH)_3(g)$ and is consequently even less stable. It is 410 kJ/mol (M) above the $ClO_3(OH)\cdot 2\ H_2O(g)$ energy minimum. This clearly demonstrates that none of the three Cl═O bonds in $ClO_3(OH)(g)$ have any affinity for hydrolytic addition of water.

The water chemistry of the Cl═O bonds is manifested in the next addition step, where proton transfer to the solvating water molecules does occur. At all levels of theory is the global energy minimum for $ClO_3(OH)\cdot 3\ H_2O(g)$ (Figure 3i), an ion pair structure which contains a $ClO_4(-)$ core bonded to an $H_3O^+\cdot 2\ H_2O$ ligand by three hydrogen bonds. The energy gain in the addition reaction is 41 (M) and 40 (L) kJ/mol. The perchlorate/hydronium ion pair thus requires the same number of water ligands to form, as does the analogous $HSO_4(-)/H_3O^+$ pair. However, in the sulfuric acid system, the ion pair structures did not represent the global energy minimum. An alternative structure is also at hand for $ClO_3(OH)\cdot 3\ H_2O(g)$, i.e., one in which the water ligands only connect to one of the Cl═O units (Figure 3h). This structure is 3−4 kJ/mol less stable than the ion pair. This fact clearly illustrates that perchloric acid is a stronger microacid than its sulfuric counterpart, in that $ClO_3(OH)(g)$ requires fewer water ligands to deprotonate on the nanoscale. The important structural contribution to ion pair formation is the three hydrogen bonds between the proton/water network and the three Cl═O units. Repeatedly, the mobility of the acidic proton as mediated by the bridging water molecules reduces the bond strain on the central ion. This can be seen from the Cl═O bond distances in the Figure 3i complex (1.46−1.54 (M) and 1.42−1.49 (L) Å), where the average bond distances become 1.50 (M) and 1.46 (L) Å. These distances correspond very neatly to those obtained for the free $ClO_4(-)$ ion, using the same basis sets. Two of the Cl═O bond distances are also equal to those of the chlorate ion. It thus can be assumed, that additional water ligands will level out the remaining differences in bond lengths between the Cl═O groups. This can be expected to occur on the nanoscale when the solvation shell around the $ClO_4(-)$ ion is completed.

$Cl_2O_7(g)$ + H_2O. Perchloric acid anhydride exists as a molecular solid.[1] The $O_3Cl-O-ClO_3$ molecule (Figure 4a) displays an energy minimum of C_2 symmetry, in which the Cl═O groups on each ClO_4 unit are rotated somewhat apart to minimize repulsion. The structural parameters are highly sensitive to the size of the basis set and, consequently, the data presented below will be those obtained using (L). For comparison to the smaller (M) basis set, those results are given in Table 4. The Cl−O−Cl bridge displays the expected 119° bond angle

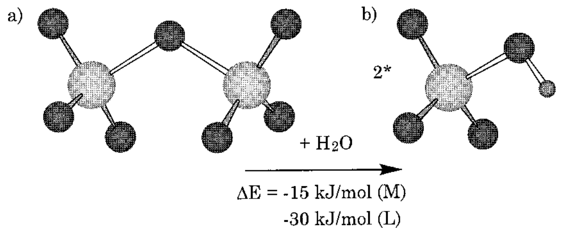

Figure 4. Structures in the Cl_2O_7 + H_2O system. Cl_2O_7: (a) $O_3ClOClO_3$ (C_2). $Cl_2O_8H_2$: (b) $2ClO_3(OH)$ (C_s), together with energetics for the hydrolysis reaction.

(L/XL), typical Cl═O bond distances (1.41−1.42 Å (L/XL)), but elongated Cl−O bonds (1.74−5 Å (L/XL)). It is gratifying to note, that these data are in good agreement with experimental findings on Cl_2O_7 (Cl−O−Cl, 119°; Cl═O, 1.42 Å; Cl−O, 1.72 Å).[23] The only shortcoming is noted for the Cl−O bond distance, which apparently is difficult to describe correctly, as it still comes out 0.02 Å too long using the (XL) basis set. The Cl−O bond in the $ClO_3(OH)$(g) monomer (Figure 4b) is significantly shorter (1.66 Å (L/XL)) than that in Cl_2O_7(g). This reflects the instability in Cl_2O_7(g), which also is observed in the exothermicity for hydrolysis of the Cl−O−Cl bridge (15 (M), 30 (L), and 31 (XL) kJ/mol). No stable water complex with Cl_2O_7(g) could be obtained, which implies that no solvation energy is associated with this species, which is in contrast to the highly solvable hydrolysis product. It is noted that the Cl−O−Cl bridge of the perchloric acid anhydride is the most pronounced high-energy anhydride of the 3p elements in the sequence Si−Cl.

Reduction of H_2SO_4(g), $HClO_4$(g), and ArO_4(g). The previous subsections addressed water addition to X═O bonds and X−O−X bridges, where water functioned both as reactant in hydrolysis and as a solvent molecule. As a third alternative, water can take the role of a reducing agent. This implies the formation of hydrogen peroxide and a reduced form of the 3p oxide species. All three species in the sequence H_2SO_4(g), $HClO_4$(g), and ArO_4(g) are known to be reducible, and it thus becomes interesting to investigate if, when and how this does occur on the nanoscale.

There are four important structures in the sulfurous acid system. Two energy minima exist for the $SO(OH)_2$(g) molecule (Figure 5b,c), in which the arrangement of the S−OH groups differ. These are separated by 3−4 kJ/mol. Another structure is the hydride, $HSO_2(OH)$(g) (Figure 5a). It is 92 (M) and 45 (L) kJ/mol less stable than the most stable $SO(OH)_2$(g) and is thus not regarded in the reduction of sulfuric acid. However, the large basis set effect is striking. What is more important is that the global energy minimum is found for $SO_2{\cdot}H_2O$(g) (Figure 5d), which is 45 (M) and 40 (L) kJ/mol below $SO(OH)_2$(g). This implies that evolution of SO_2(g) becomes energetically favored when sulfurous acid is formed, and this must be remembered when reduction is discussed. The present study though concentrates on the two types of $SO(OH)_2{\cdot}H_2O_2$(g) complexes (Figure 1f and 1g) that can be formed when water is used to reduce H_2SO_4(g). The two structures differ by the way the OH units bind to H_2O_2. The complex in Figure 1f has hydrogen bonds only between the S−OH groups and H_2O_2, whereas the structure in Figure 1g has one of the H bond directed toward the S═O group. This difference renders the latter complex 9 kJ/mol (M) lower energy. Compared to the $SO_2(OH)_2{\cdot}H_2O$(g) complex in Figure 1i, the reduced $SO(OH)_2{\cdot}H_2O_2$(g) structure in Figure 1g is 205 (M) and 279 (L) kJ/mol less stable. The large basis set effect on the energetics for the reduction indicates that the (M) basis set is insufficient for correctly describing the process. The reason for this is that an accurate description of the S═O and S−OH bonds requires a very large basis set on S. As the number of such bonds is changed when $SO_2(OH)_2$(g) is reduced to $SO(OH)_2$(g), this reaction becomes highly sensitive to these effects. The error that appears in this first reduction step is as large as 75 kJ/mol. The energetics for processes that preserve the oxidation state on S are much less affected by a sub-optimal description. Still, the conclusion that can be drawn from the calculations is that water alone cannot reduce H_2SO_4, despite the fact that some additional energy is gained when $SO_2{\cdot}H_2O$(g) is formed. Instead, water addition to one of the S═O bonds in $SO_2(OH)_2$(g) becomes more favored, despite the fact that this reaction also constitutes an endothermic process.

The stability of $SO_2(OH)_2$(g) can be evaluated further by studying some alternative reduction routes. Direct decomposition of sulfuric acid to H_2S(g) by oxygen evolution is thus an energetically unfavorable path:

$$SO_2(OH)_2(g) \rightarrow H_2S(g) + 2O_2(g) \quad \Delta E = +420 \text{ kJ/mol (M)} \quad +598 \text{ kJ/mol (L)} \tag{R7}$$

To reduce the acid to H_2S(g), a suitable reducing agent is needed. One such candidate is H_2(g):

$$SO_2(OH)_2(g) + 4H_2(g) \rightarrow H_2S(g) + 4H_2O(g) \quad \Delta E = -466 \text{ kJ/mol (M)} \quad -288 \text{ kJ/mol (L)} \tag{R8}$$

It can consequently be concluded that the reduction of H_2SO_4 requires a reducing agent of equivalent power to H_2(g). From the reaction energetics in R7 and R8, it can be seen that the total error in the energies of the reduction processes when using (M) is 178 kJ/mol. This discrepancy is significant and calls for caution when evaluating energetics obtained using too small basis sets.

Reduction of perchloric acid by molecular water results in the formation of the $ClO_2(OH){\cdot}H_2O_2$(g) complex (Figure 3c). The reaction from $ClO_3(OH){\cdot}H_2O$(g) is exothermic by 17 kJ/mol using the (M) basis set but endothermic by 74 kJ/mol using (L). Again, the discrepancy is a result of the error caused by the use of an incomplete basis set. It can be noted that there are two minimum structures for chloric acid. The global energy minimum contains the oxyhydroxide $ClO_2(OH)$(g) (Figure 5f), but in addition to this species, there is the $HClO_3$(g) molecule (Figure 5e), i.e., the hydride, which has C_{3v} symmetry. The latter species lies 262 (M) and 183 (L) kJ/mol above the former, which

TABLE 4: Summaries of Bond Lengths *R* (Å) and Bond Angles *A* (deg) and Ranges of Vibrational Frequencies (cm^{-1}), Together with Normal-Mode Symmetries and the Number of Vibrations in Each Group, for the Cl_2O_7 + nH_2O Systems

		$O_3ClOClO_3$		
C_2	R(Cl═O): 1.452−1.455	A(O═Cl═O): 115.0−115.8	A(Cl−O−Cl): 120.8	A + B (11+10 vib.): 26−1165
(M)	R(Cl−O): 1.805	A(O═Cl−O): 97.5−105.2		
C_2	R(Cl═O): 1.412−1.416	A(O═Cl═O): 115.0−115.8	A(Cl−O−Cl): 119.3	A + B (11+10 vib.): 22−1308
(L)	R(Cl−O): 1.746	A(O═Cl−O): 97.6−105.0		

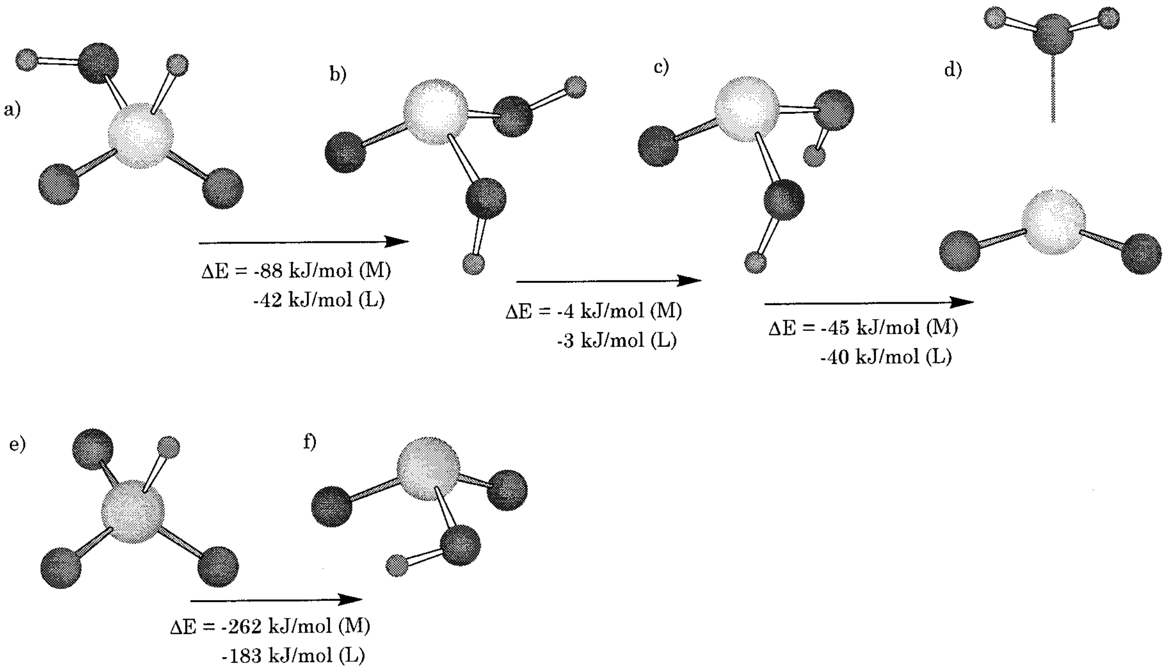

Figure 5. Structures for $SO(OH)_2$ and $ClO_2(OH)$: (a) $HSO_2(OH)(g)$ (C_1), (b and c) $SO(OH)_2(g)$ (C_1 and C_s), (d) $SO_2{\cdot}H_2O(g)$ (C_1), (e) $HClO_3(OH)(g)$ (C_{3v}), and (f) $ClO_2(OH)(g)$ (C_1), together with relative stabilities.

TABLE 5: Summaries of Bond Lengths *R* (Å) and Bond Angles *A* (deg) and Ranges of Vibrational Frequencies (cm^{-1}), Together with Normal-Mode Symmetries and the Number of Vibrations in Each Group, for the $ArO_4 + nH_2O$ System

		ArO_4	
T_d (M)	$R(Ar{=}O)$: 1.574	$A(O{=}Ar{=}O)$: 109.5	$A_1 + E + T_2$ (1+1+2 vib.): 296−704
T_d (L)	$R(Ar{=}O)$: 1.472	$A(O{=}Ar{=}O)$: 109.5	$A_1 + E + T_2$ (1+1+2 vib.): 395−928
T_d (XL)	$R(Ar{=}O)$: 1.470	$A(O{=}Ar{=}O)$: 109.5	$A_1 + E + T_2$ (1+1+2 vib.): 399−937
		ArO_3	
C_{3v} (M)	$R(Ar{=}O)$: 1.647	$A(O{=}Ar{=}O)$: 111.7	$A_1 + E$ (2+2 vib.): 275−606
C_{3v} (L)	$R(Ar{=}O)$: 1.514	$A(O{=}Ar{=}O)$: 110.1	$A_1 + E$ (2+2 vib.): 387−851
C_{3v} (XL)	$R(Ar{=}O)$: 1.511	$A(O{=}Ar{=}O)$: 110.0	$A_1 + E$ (2+2 vib.): 395−864
		ArO_2	
C_{2v} (M)	$R(Ar{-}O)$: 1.776	$A(O{-}Ar{-}O)$: 124.2	$A_1 + B_2$ (2+1 vib.): 202−497
C_{2v} (L)	$R(Ar{-}O)$: 1.630	$A(O{-}Ar{-}O)$: 122.2	$A_1 + B_2$ (2+1 vib.): 275−690
C_{2v} (XL)	$R(Ar{-}O)$: 1.621	$A(O{-}Ar{-}O)$: 121.5	$A_1 + B_2$ (2+1 vib.): 268−711
		ArO	
$C_{\infty v}$ (M)	$R(Ar{-}O)$: 1.911		sg (1 vib.): 418
$C_{\infty v}$ (L)	$R(Ar{-}O)$: 1.803		sg (1 vib.): 449
$C_{\infty v}$ (XL)	$R(Ar{-}O)$: 1.788		sg (1 vib.): 461

excludes the hydride from the present considerations. However, the large basis set effect is noteworthy, and its size can be connected with the large energy separation between the hydroxide and the hydride. The relative instability if the hydride is another manifestation of the general instability of the Cl=O bond (one more than in the hydroxide). The binding energy of $H_2O_2(g)$ to $ClO_2(OH)(g)$ is found to be 35 (M) and 33 (L) kJ/mol, which is too small to alter the sign of the reduction energetics. It is also clear that the fact that no simple reaction path connects the $ClO_3(OH){\cdot}H_2O(g)$ complex with the chloric acid + hydrogen peroxide complex effectively hinders the reduction. Although water might work as a reducing agent for perchloric acid, the onward reaction HCl(g) is clearly endothermic:

$$ClO_3(OH)(g) + 4H_2O(g) \rightarrow HCl(g) + 4H_2O_2(g) \quad \Delta E = +32 \text{ kJ/mol (M)} \quad +279 \text{ kJ/mol (L)} \tag{R9}$$

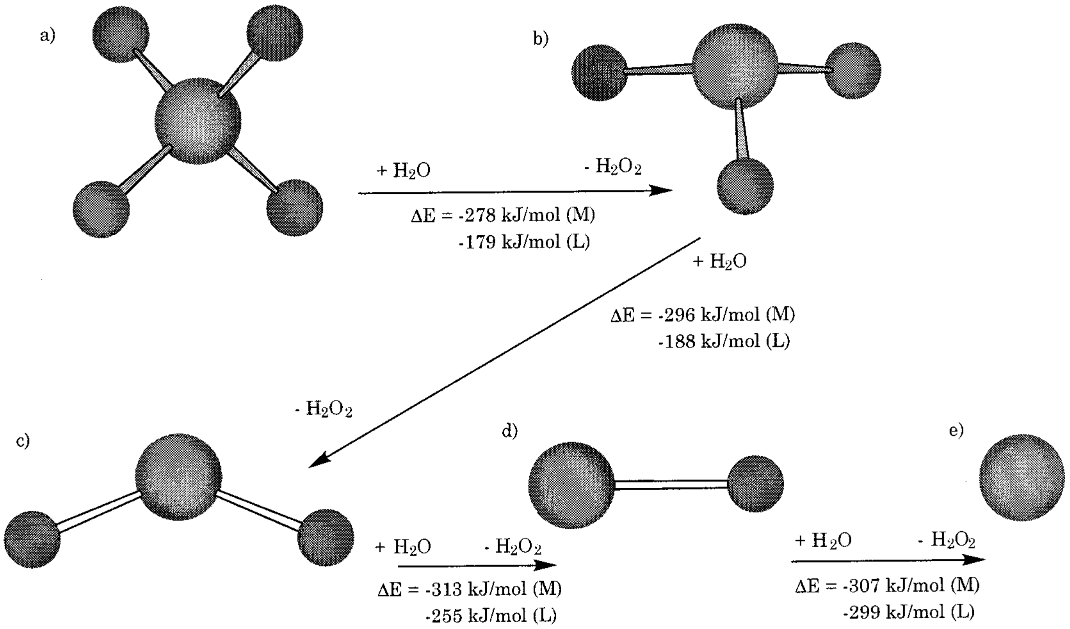

Figure 6. Structures in the $ArO_4 + 4\ H_2O$ system: (a) ArO_4 (T_d), (b) ArO_3 (C_{3v}), (c) ArO_2 (C_{2v}), (d) ArO ($C_{\infty v}$), and (e) Ar, together with energetics for the hydrolysis reactions.

Direct decomposition of perchloric acid constitutes the simplest route to HCl(g) and is accompanied by oxygen evolution:

$$ClO_3(OH)(g) \rightarrow HCl(g) + 2O_2(g) \quad \Delta E = -439 \text{ kJ/mol (M)} \quad -193 \text{ kJ/mol (L)} \quad -194 \text{ kJ/mol (XL)} \quad \text{(R10)}$$

Despite the 247 kJ/mol basis set effect on reaction energetics, this reaction is still clearly exothermic. The only effect that can alter this is the condensation energy for $ClO_3(OH)(g)$ in comparison with that for HCl(g). The formation of $O_2(g)$ also put constraints on the reaction route in R10, and in general, a catalyst is required for the reduction to occur. When comparing the exothermicities obtained using the (L) and (XL) basis sets, it becomes clear that the (L) set is enough for a correct description of the reduction process.

The exotic $ArO_4(g)$ molecule (Figure 6a) is an isoelectronic analogue to $SO_2(OH)_2(g)$ and $ClO_3(OH)(g)$, in which Ar diplays the same number of bonds in the valence as the tetrahedral $FeO_4(g)$. The latter molecule has been investigated theoretically, but it is only its much more stable isomers (e.g., $Fe(O_2)_2(g)$) that have been observed experimentally.[24] There has previously been some theoretical studies on $ArO_4(g)$, as well as other Ar oxides, in the literature,[25-27] but no unambiguous experimental results exist. Hence, although $ArO_4(g)$ itself is a stable species, which displays four equivalent Ar=O bonds (1.57 (M) and 1.47 (L) Å) in a tetrahedral arrangement, the reaction with $H_2O(g)$ to form $ArO_3(g)$ (Figure 6b) and $H_2O_2(g)$ proceeds directly without any detectable intermediary species or transition state. In this reduction, as much as 278 (M) and 179 (L) kJ/mol are released. The obvious reason for this instability is found in the fact that Ar lacks the flexibility in the valence to form four Ar=O bonds, which are competitive to O=O bonding. Another point of interest is the very large basis set effect on bond distances and energetics for $ArO_4(g)$. It is obvious, that the 6-311+G(d,p) basis set (M) is insufficient for obtaining any valid description of Ar oxides, but that very good results can be obtained by expanding the basis set. As can be seen from Table 5, proper bond lengths are calculated when the basis set on Ar is expanded to 6-311+G(3df) (L), while only minor changes are noted on expanding the basis set on O further to 6-311+G(3df) (XL). Besides the fact that B3LYP, using the larger basis sets, is able to reproduce the bond distances obtained at coupled cluster levels, it performs equally well at reaction energetics. When comparing the exothermicity of the isodesmic reaction used by Lindh et al.[26] to the present results (reaction 9), it becomes obvious that B3LYP/6-311+G(3df) performs just as well as does the much more expensive CCSD(T)/ANO method:

$$ArO_4(g) + Cl^-(g) \rightarrow Ar(g) + ClO_4^-(g) \quad \Delta E = -1328 \text{ kJ/mol (XL)} \quad \text{(R11)}$$

When the DFT reaction energies for R11, presented in ref 26, are recalculated from the tabulated total energies, given in this reference, the results cannot be reproduced. Due to the mixup of B3LYP and BP86 values, the accuracy of DFT is underestimated, in comparison to the other methods used in ref 26.

The pyramidal $ArO_3(g)$ reacts with $H_2O(g)$ in a similar fashion, giving $ArO_2(g)$ (Figure 6c) and $H_2O_2(g)$. The lone pair on the Ar atom hinders all bonding to the free coordination site on this electronically depleted atom, and hence, no water complex is formed. The lability of $ArO_3(g)$ is illustrated by the three elongated Ar=O bonds (1.65 (M) and 1.51 (L) Å). The reduction process is exothermic by 296 (M) and 188 (L) kJ/mol. The bent $ArO_2(g)$ molecule has two long Ar−O bonds (1.78 (M) and 1.63 (L) Å), where two Ar=O bonds would be expected, which again is an indicator on its oxidating power. In accordance, the reaction with $H_2O(g)$ and subsequent formation of ArO(g) (Figure 6d) and $H_2O_2(g)$ release 313 (M) and 255 (L) kJ/mol. This, the smallest Ar oxide displays a very long Ar−O bond (1.91 (M) and 1.80 (L) Å), and the O atom is thus only weakly bound to Ar. The reactivity toward $H_2O(g)$, forming the free Ar atom and $H_2O_2(g)$, matches those above as 307 (M) and 299 (L) kJ/mol is released. In total, the reduction of $ArO_4(g)$ by four water molecules becomes exothermic by 921 kJ/mol (L), which supports the rareness of Ar oxides in nature. The reduction of ArO4(g) through direct oxygen evolution is also a highly exothermic process:

$$ArO_4(g) \rightarrow Ar(g) + 2O_2(g) \qquad \Delta E = -1678 \text{ kJ/mol (M)}$$
$$-1393 \text{ kJ/mol (L)}$$
$$-1389 \text{ kJ/mol (XL)} \qquad \text{(R12)}$$

Similar to perchloric acid though, there is a need for a catalyst for this direct reaction to occur.

Conclusions

The energetics and structures of the oxides and oxyhydroxides of S, Cl, and Ar in the present investigation turn out to be highly sensitive to choice of basis set in the calculations. The popular 6-311+G(d,p) basis set (M) is found to give X−O bond distances that are too long and, in particular, unreliable reaction energies for redox processes. The results are greatly improved if the basis set on S, Cl, and Ar is extended to the large 6-311+G(3df) set (L). B3LYP calculations, using this larger basis set, are found to give results of equal quality to the much more expensive CCSD(T) method. In the following, only data obtained with the (L) basis set are discussed, as they are the most reliable.

The addition of water to $SO_3(g)$ is found exothermic by 62 kJ/mol. This rather small value is contrasted by the fact that the addition product of $SO_3(g)$ and four water molecules, the $SO_2(OH)_2 \cdot 3\ H_2O$ complex, spontaneously deprotonates and forms an ion pair. The formation of a hydronium ion clearly illustrates that this system indeed comprises a strong acid, although the ion pair is slightly above (6 kJ/mol) the protonated global energy minimum. The cause of this acidity is found in the instability of the local S═O bonds. The core S atom can neither support full covalency in all bonds nor support the highly ionic alternative. Water ligands introduce the option of proton loss, and the only requirement is that three out of four O atoms are interconnected through hydrogen bonds. The same effect is observed for the $ClO_3(OH)$ system, which represents an extremely strong Brønsted acid. Three water ligands are required to deprotonate this acid too. The conclusion on these facts, given that $PO(OH)_3$ acts as a weak acid, is that the 3p elements can support four covalent bonds in combination with the equivalent of one ionic bond. If the demand for covalent bonding is pushed higher, the systems become unstable. One dominant manifestation of this instability is the tendency for proton transfer. Another indicator for instability is found in reduction processes, either through O_2 evolution or by using H_2 as a reducing agent. While $ClO_3(OH)(g)$ displays exothermicity for decomposition into HCl(g) and 2 $O_2(g)$, an equivalent of H_2 is needed in order to reduce the sulfuric acid system to $H_2S(g)$. For the $ArO_4(g)$ extreme, the reduction by water becomes spontaneous.

Cleavage of the S−O−S and Cl−O−Cl bridges in $S_2O_7H_2$ and Cl_2O_7 is exothermic by 23−30 kJ/mol for both systems. When comparing this result to the Si and P systems, it is clear that the S and Cl systems contain bonds that on a relative scale can be considered as “high-energy bonds” toward hydrolysis. However, the critical parameter for the stability of such bridges is the water content. Under dry conditions, polymerization will be a favorable route. This is most clearly pronounced in concentrated sulfuric acid, which turns highly viscous due to chain formation. This acid is simultaneously extremely hygroscopic, an effect that originates in the stability of the hydrates. Finally, the instability of the local S═O and Cl═O bonds is responsible for the acidity of sulfuric and perchloric acid.

Acknowledgment. This work was supported by the Swedish Natural Sciences Research Council (NFR). The National Supercomputer Center (NSC) in Linköping is acknowledged for allotment of computer time.

Supporting Information Available: Tables listing detailed structural parameters, absolute energies, and vibrational frequencies (47 pages). This material is available free of charge via the Internet at http://pubs.acs.org.

References and Notes

(1) Greenwood, N. N.; Earnshaw, A. *Chemistry of the Elements*, 2nd ed.; Butterworth-Heinemann: Oxford, 1997.
(2) Johnson, J. R. T.; Panas, I. *Phys. Chem. Chem. Phys.*, in press.
(3) Johnson, J. R. T.; Panas, I. *Chem. Phys.*, in press.
(4) Johnson, J. R. T.; Panas, I. *Inorg. Chem.* **2000**, *39*, 3181
(5) Johnson, J. R. T.; Panas, I. *Inorg. Chem.* **2000**, *39*, 3192
(6) Becke, A. D. *J. Chem. Phys.* **1993**, *98*, 5648
(7) Johnson, J. R. T.; Panas, I. *Chem. Phys.* **1999**, *248*, 161
(8) Bauschlicher, C. W.; Zhou, M.; Andrews, L.; Johnson, J. R. T.; Panas, I.; Snis, A.; Roos, B. O. *J. Chem. Phys. A* **1999**, *103*, 5463. Further details on the ScO_2 system in: Johnson, J. R. T. Structure and Bonding in 3d and 4p Metal Oxide Clusters. Licentiate thesis, Göteborg University (S), Götenborg, Sweden, 1999.
(9) Johnson, J. R. T.; Panas, I. *Chem. Phys.* **1999**, *249*, 273
(10) Frisch, M. J.; Trucks, G. W.; Schlegel, H. B.; Scuseria, G. E.; Robb, M. A.; Cheeseman, J. R.; Zakrzewski, V. G.; Montgomery, J. A., Jr.; Stratmann, R. E.; Burant, J. C.; Dapprich, S.; Millam, J. M.; Daniels, A. D.; Kudin, K. N.; Strain, M. C.; Farkas, O.; Tomasi, J.; Barone, V.; Cossi, M.; Cammi, R.; Mennucci, B.; Pomelli, C.; Adamo, C.; Clifford, S.; Ochterski, J.; Petersson, G. A.; Ayala, P. Y.; Cui, Q.; Morokuma, K.; Malick, D. K.; Rabuck, A. D.; Raghavachari, K.; Foresman, J. B.; Cioslowski, J.; Ortiz, J. V.; Stefanov, B. B.; Liu, G.; Liashenko, A.; Piskorz, P.; Komaromi, I.; Gomperts, R.; Martin, R. L.; Fox, D. J.; Keith, T.; Al-Laham, M. A.; Peng, C. Y.; Nanayakkara, A.; Gonzalez, C.; Challacombe, M.; Gill, P. M. W.; Johnson, B.; Chen, W.; Wong, M. W.; Andres, J. L.; Gonzalez, C.; Head-Gordon, M.; Replogle, E. S.; Pople, J. A. *Gaussian 98*, Revision A.6; Gaussian, Inc.: Pittsburgh, PA, 1998.
(11) Chase, M. W., Jr.; Davies, C. A.; Downey, J. R., Jr.; Frurip, D. J.; McDonald, R. A.; Syverud, A. N. *J. Phys. Chem. Ref. Data* **1985**, *14*, Suppl. 1
(12) Givan, A.; Larsen, L. A.; Loewenschuss, A.; Nielsen C. J. *J. Chem. Soc., Faraday Trans.* **1998**, *94*, 827
(13) Meijer, E. J.; Sprik, M. *J. Phys. Chem. A* **1998**, *102*, 2893
(14) Larson, L. J.; Kuno, M.; Tao, F.-M. *J. Chem. Phys.* **2000**, *112*, 8830
(15) Re, S.; Osamura, Y.; Morokuma, K. *J. Phys. Chem. A* **1999**, *103*, 3535
(16) Kuczkowski, R. I.; Suenram, R. D.; Lovas, F. J. *J. Am. Chem. Soc.* **1981**, *103*, 2561
(17) Bandy, A. R.; Ianni, J. C. *J. Phys. Chem. A* **1998**, *102*, 6533
(18) McKee, M. L. *J. Phys. Chem.* **1996**, *100*, 3473
(19) Hönle, W. *Z. Kristallogr.* **1991**, *196*, 279
(20) Ianni, J. C.; Bandy, A. R. *J. Mol. Struct. (THEOCHEM)* **2000**, *497*, 19
(21) Casper, B.; Mack, H. G.; Muller, H. S. P.; Willner, H.; Oberhammer, H. *J. Phys. Chem.* **1994**, *98*, 8339
(22) Weber, K. H.; Tao, F.-M. *J. Phys. Chem. A* **2001**, *105*, 1208
(23) Simon, A.; Borrmann, H. *Angew. Chem., Int. Ed. Engl.* **1988**, *27*, 1339
(24) Chertihin, G. V.; Saffel, W.; Yustein, J. T.; Andrews, L.; Neurock, M.; Ricca, A.; Bauschlicher, C. W. *J. Phys. Chem.* **1996**, *100*, 5261
(25) Pyykkö, P. *Phys. Scr.* **1990**, *T33*, 52
(26) Lindh, R.; Kraemer, W. P.; Kamper, M. *J. Phys. Chem. A* **1999**, *103*, 8295
(27) Pyykkö, P. *Chem. Eur. J.* **2000**, *6*, 2145